

## Estimation of Frequency Reserves Requirement & Evaluation of BESS Dispatch Strategy for the 2030 Italian Electricity Market

TESI MAGISTRALE IN ENERGY ENGINEERING

**USAMA, CH MUHAMMAD**

**Advisor:**

Giuliano Rancilio

**Co-advisor:**

Diego Andreotti

**Academic year:**

2024-25

**Abstract:** In power systems with high shares of non-programmable renewable energy sources (NPRES), balancing generation and demand and ensuring frequency stability becomes increasingly complex. Reduced system inertia and variability in renewable output call for flexible resources capable of providing rapid frequency reserves and absorbing excess energy. This study investigates the role of Battery Energy Storage Systems (BESS) in supporting the Italian power system in 2030 through two services: time-shifting and frequency reserve provision. To estimate future reserve needs, two methodologies (formula-based and convolution-based) are applied using historical forecast error matrices for load, solar, and wind generation. Results show a substantial increase in reserves from 2023 to 2030. Under the formula method, upward reserve requirements grow by 20% and downward by 62%, while the convolution method estimates an increase of 12% for upward and 31% for downward reserves. The modeled BESS fleet, sized according to Italy 2030 NECP targets, operates on a price-based dispatch strategy. Results show the system delivers approximately 214 full cycles annually for RES time-shifting and it is available to provide 50% of upward and 79% of downward reserves. Time-shifting performance reveals 11 TWh of energy discharged for peak shaving, demonstrating significant load flexibility during high-price events. BESS coverage peaks in spring and autumn, with over 90% downward reserve participation in certain months, and it contributes more during weekdays than weekends due to higher demand and stronger price signals. An economic evaluation suggests that the total reserve provision costs amount to approximately €185 million per year. The share attributed to BESS, considering its portion of activated reserves, amounts to €66 million per year. These findings highlight the strategic role of BESS as a dual-purpose asset capable of providing both energy arbitrage and ancillary services. The results of this study offer valuable insights for policymakers to refine market designs and ensure grid stability in high-renewable energy scenarios.

**Key-words:** frequency reserve estimation; battery energy storage system (BESS); charging and discharging strategy; RES time shifting; Italy 2030 NECP; high renewable integration

## 1. Introduction

The ongoing decarbonization of the power sector is driving a rapid transformation of electricity systems worldwide, with renewable energy sources (RES) like solar and wind becoming increasingly dominant in generation portfolios [1]. While this transition supports climate goals, the integration of non-dispatchable renewable sources introduces significant variability and uncertainty into the power grid [2]. These forecast errors challenge the conventional mechanisms used to maintain system balance, particularly in real-time operations. To ensure grid reliability, system operators must maintain sufficient reserves that can respond to unexpected fluctuations in generation or demand [3]. As traditional thermal power plants gradually phase out, Battery Energy Storage Systems (BESS) are emerging as a key enabler of system flexibility, capable of both absorbing excess energy and injecting power during shortfalls. In this context, accurately estimating reserve requirements and quantifying the potential contribution of BESS especially under market-driven operation and forecast uncertainty becomes essential for the secure and efficient operation of future power systems such as that of Italy in 2030 [4].

In modern power systems, reserves are deployed across different response timescales to maintain system stability amidst variability and uncertainty, particularly from renewable generation. These reserves are typically structured into three categories: primary, secondary, and tertiary reserves. Primary reserves, commonly referred to as Frequency Containment Reserves (FCR) are automatically activated within seconds to counteract frequency deviations. Secondary reserves, known as Automatic Frequency Restoration Reserves (aFRR), intervene within a few minutes to restore system frequency to its nominal value. Tertiary reserves, such as Manual Frequency Restoration Reserves (mFRR), provide slower but sustained support through manual activation and are further divided into spinning and non-spinning components depending on their readiness for dispatch [5]. Accurately estimating these reserve requirements is crucial, especially under increasing renewable penetration and declining inertia. To this end, different methodologies can be employed, including deterministic formulas or probabilistic approaches like convolution-based techniques, each with varying assumptions about forecast uncertainty. Moreover, integrating BESS into reserve provision adds a new layer of operational flexibility. BESS can dynamically participate in both upward and downward reserves, making them particularly suited for balancing fluctuations in net load due to solar and wind variability [6].

As Italy advances towards its 2030 National Energy and Climate Plan (NECP) objectives, aiming for renewables to contribute over 65% of electricity consumption, the integration of BESS becomes increasingly pivotal [7]. The anticipated rise in non-programmable renewable energy sources (NP-RES), such as wind and solar, introduces significant variability and uncertainty into the power grid [8]. This variability necessitates enhanced flexibility and rapid response mechanisms to maintain grid stability. BESS, with their ability to provide fast-response power, are well-suited to address these challenges by offering services like frequency regulation and load balancing. Italy's commitment to expanding its energy storage capacity, targeting 50 GWh of grid-scale energy storage by 2030, underscores the strategic importance of these systems in the nation's energy transition. Accurately estimating reserve requirements and understanding the potential contributions of BESS are thus essential for ensuring both the reliability and efficiency of Italy's future power system [7]. The responsibility for estimating reserve requirements typically falls on Transmission System Operators (TSOs), who must ensure that sufficient reserves are available to balance the system in real time. Traditionally, reserve dimensioning has relied on deterministic rules, often based on peak load or worst-case contingencies. However, with the increasing penetration of NP-RES, these static methods are proving inadequate. As a result, many European TSOs have shifted towards

probabilistic or dynamic reserve estimation strategies. For example, German TSOs employ statistical convolution methods with high confidence intervals (e.g. 99.95%) to determine reserve needs under uncertainty, ensuring robust margins against renewable variability and load forecast errors [9]. In contrast, Belgium has introduced machine learning models to dynamically predict reserve requirements, adapting reserve levels based on real-time system conditions and thereby reducing over-procurement [10].

Recent research in Spain and Portugal proposed a probabilistic reserve evaluation approach for systems with high wind penetration, capturing the inherent uncertainty in generation [11]. Beyond Europe, recent advancements in deep learning techniques such as LSTM and GRU neural networks have shown great promise in reducing forecast errors for both load and RES output, enabling more accurate reserve allocation [12]. These techniques have been successfully demonstrated in countries like China and South Korea, where TSOs have integrated near real-time data and AI forecasting to minimize deviations and improve operational efficiency.

In this evolving landscape, BESS emerges as a critical asset. BESS can offer fast and flexible ramping capabilities, providing synthetic inertia, frequency regulation, and both upward and downward reserves. Several studies have confirmed that incorporating BESS into reserve planning significantly reduces the total reserve requirements and operational costs, particularly in systems with high-RES shares. Moreover, BESS can help absorb excess renewable generation during low-demand periods and discharge during deficits, effectively acting as a dynamic buffer. Hence, future reserve dimensioning frameworks must not only rely on probabilistic error modeling and forecast enhancement but also explicitly account for the contribution of BESS to optimize reserve procurement and ensure grid stability in high-renewable scenarios [13].

To determine the appropriate quantity of reserves required, two main approaches are commonly used: the empirical (formula-based) method and the convolution-based probabilistic method. The empirical method estimates reserve needs through structured formulas derived from historical trends and system-specific parameters, offering a transparent and widely adopted approach particularly suited for secondary reserves. In contrast, the convolution method adopts a probabilistic framework, incorporating the statistical distributions of forecast errors in load, solar, and wind generation. This enables a more precise representation of system uncertainty, especially valuable for accurately estimating tertiary reserve needs in systems with high renewable penetration. While the empirical method ensures regulatory alignment and simplicity, the convolution approach captures the stochastic nature of forecast variability more effectively, making both methodologies complementary in evaluating system flexibility requirements [14].

In this study, the Italian power system is analyzed under the lens of increasing renewable energy integration in line with the 2030 NECP. Reserve requirements for both 2023 and 2030 are estimated using empirical and convolution methods, using forecast error matrices for solar, wind and load using historical data. This forward-looking framework better reflects the uncertainty present at the time of system operation planning. Additionally, a detailed analysis is conducted on the role of BESS in supporting grid reliability through RES time-shifting. Based on simulated battery operation under projected 2030 market conditions, the study evaluates the real-time state-of-charge (SOC), charging and discharging profiles, and their alignment with reserve demand. The contribution of BESS to both upward and downward reserves is quantified and assessed against total system needs, offering critical insights into how energy storage can complement traditional reserves in managing renewable intermittency. This integrated approach not only enhances the accuracy of reserve sizing but also highlights the operational value of flexible resources in future high renewable scenarios.

## 1.1 Research Question

As EU Green Deal pushes for low-emitting power systems by 2030, the increasing share of variable renewable energy sources introduces increased uncertainty in power system operation, especially in forecasting load, wind, and solar generation. This growing uncertainty poses critical challenges for system operators in determining accurate reserve requirements and assessing the reliability of flexible resources such as BESS. Despite advances in forecasting and storage technologies, there remains a research gap in understanding how empirically derived reserve estimation methods interact with economically optimized storage operation. This study seeks to address the central question: How can improved reserve estimation methodologies, paired with realistic BESS dispatch strategies, inform system operation on hourly estimated contribution of BESS for operational security? By doing so, the research contributes to ongoing discussions on future reserve sufficiency, the economic role of storage, and the integration of emerging flexibility mechanisms into planning frameworks.

## 1.2 Novelty

The novelty of this study lies in its integrated approach that combines reserve requirement estimation with the operational modeling of BESS using a real-world pricing strategy for 2030. While previous studies primarily focus on reserve sizing or battery economics in isolation, this research bridges the two domains by (i) quantifying reserve needs using both formula and convolution methods under forecast uncertainty, and (ii) evaluating the practical coverage potential of BESS based on an optimized charging and discharging profile derived from energy price signals. Furthermore, the thesis presents a detailed monthly and weekday/weekend analysis of reserve coverage, equivalent battery cycles, energy throughput, and economic impacts, offering insights into system flexibility. This multidimensional perspective provides policymakers and TSOs with an evidence-based framework to align reserve planning with BESS market integration and upcoming regulatory mechanisms like the TIDE reform [15].

## 2. Methodology

This study estimates system reserves by combining empirical formulations and probabilistic modeling, reflecting operational uncertainty under high renewable penetration. Spinning reserves (aFRR and mFRR) are calculated using ENTSO-E<sup>1</sup> compliant formula methods based on load dynamics and ramping behavior [5]. Non-spinning tertiary reserves are evaluated using both a formula-based approach and a convolution-based probabilistic method [14]. Forecast error matrices for load, wind, and solar generation are applied during the reserve calculations. All estimations are performed for the years 2023 and 2030 using forecast data. Figure 1 presents an overview of the study methodology. It begins with the collection of essential input data, including forecasted load and generation profiles, historical forecast error matrices for load, wind, and solar, BESS technical parameters, and electricity market price projections for 2030. Based on these inputs, the study proceeds along two parallel tracks. On one side, the reserve requirements for 2023 and 2030 are estimated using both formula-based and convolution-based methodologies, covering secondary (aFRR), spinning tertiary (mFRR), and non-spinning tertiary reserves. On the other side, a BESS dispatch model is developed that prioritizes energy time-shifting, in alignment with MACSE guidelines. Only after satisfying the profitability conditions for time-shifting is the residual capacity

---

<sup>1</sup> ENTSO-E (European Network of Transmission System Operators for Electricity) represents 39 TSOs across 35 European countries, ensuring grid security and reliability through common operational and regulatory frameworks, including reserve estimation methodologies.

assessed for reserve provision. The final step evaluates the extent to which the BESS is able to contribute to upward and downward reserves for each hour in the year 2030 offering both a technical and economic perspective on its role in supporting grid stability.

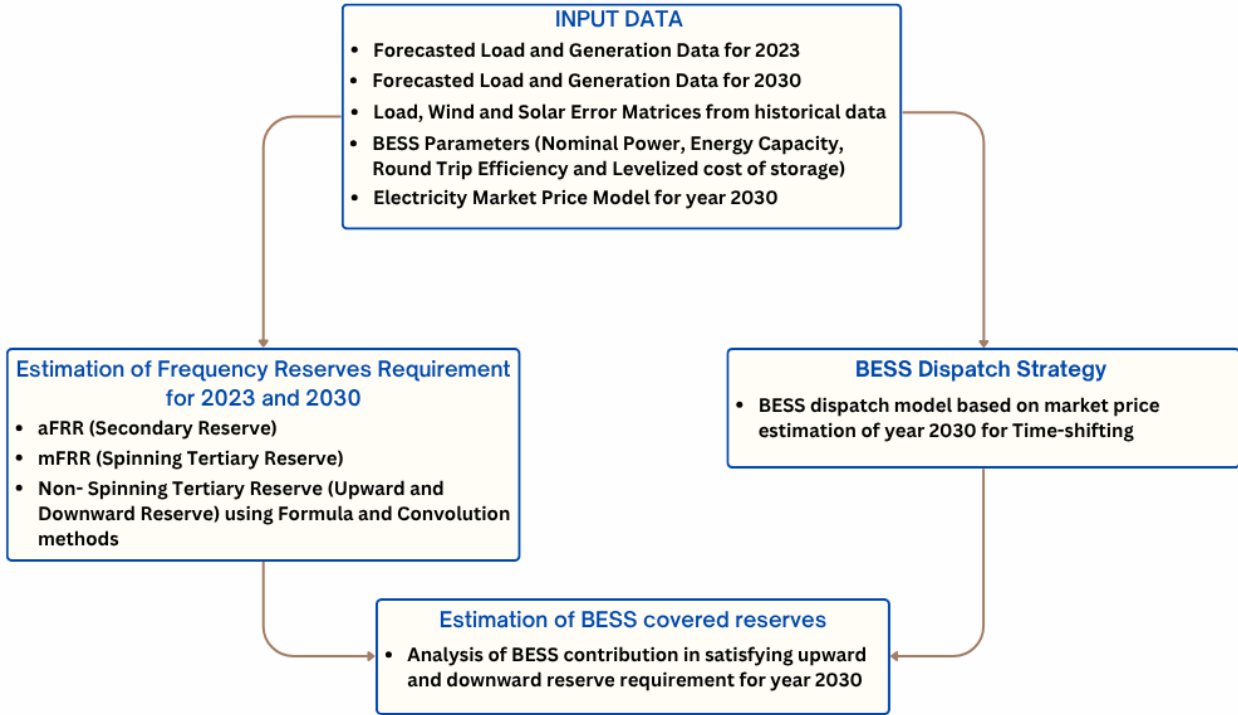


Figure 1. Overall methodological approach

## 2.1 Automatic Frequency Restoration Reserve (aFRR) Calculation

The aFRR requirement is derived using the following empirical eq.(1):

$$aFRR_{k,i} = \sqrt{a * L_{max,k,i} + b^2} - b \quad (1)$$

Where:

- $L_{max,k,i}$  represents the maximum forecasted system load for each time interval,
- $a$  is a system-dependent coefficient that scales the reserve requirement based on historical data, and  $a$  is taken as 10 MW.
- $b$  is an adjustment factor ensuring adequate response capability, and  $b$  is taken as 150MW.

This formulation ensures that aFRR provides an automated correction mechanism for sudden load fluctuations, maintaining system frequency stability by activating reserves within seconds to minutes.

## 2.2 Manual Frequency Restoration (mFRR) Calculation

The mFRR requirement accounts for longer-term imbalances and is based on the load ramping rate, ensuring sufficient reserves to compensate for changes that cannot be addressed by aFRR alone. The reserve is calculated using eq.(2) and eq.(3).

$$mFRR_{k,i} = aFRR_{k,i} * (1 + |LoadRamp_{k,i}|) \quad (2)$$

$$LoadRamp_{k,i} = \left| \frac{L_i - L_{i-1}}{L_i} \right| \quad (3)$$

Where:

- $L_i$  and  $L_{i-1}$  represent the residual load at consecutive time steps.
- The term  $\frac{L_i - L_{i-1}}{L_i}$  represents the maximum observed load ramping rate over the dataset.

These equations ensure that the mFRR reserve scales dynamically with grid variations, providing a flexible mechanism to restore balance following disturbances that exceed aFRR capabilities. The empirical method was applied to both 2023 and 2030 datasets to estimate spinning reserves under evolving grid conditions. Instead of relying on retrospective actual-forecast differences, forecast uncertainty was modeled using percentage error matrices derived from historical analysis (2017-2019) presented in Bovera et al. [5]. These error matrices applied to forecasted load, wind, and solar values enabled a forward-looking reserve estimation approach that reflects uncertainty inherent in system planning. Reserve needs for 2030 were then projected using the updated demand and renewable profiles defined by NECP target of Italy.

### 2.3 Non-Spinning Tertiary Reserve Calculation

Non-spinning tertiary reserves provide additional system flexibility by managing imbalances that are beyond the capability of spinning reserves. Unlike aFRR and mFRR, which are synchronized with the grid and respond in real time, non-spinning reserves must be activated manually or automatically before they can be used. These reserves are separated into upward and downward components: upward reserves cover situations where generation must be increased or demand reduced, while downward reserves are used when generation needs to be reduced or demand increased.

In this study, the reserve requirement is calculated by considering the forecast uncertainty in load, wind, and solar generation, along with assumptions about the largest single power plant outage. The estimation uses a 99.7% confidence level, corresponding to a 2.74 multiplier, to account for extreme but plausible system variations.

#### 2.3.1 Upward Non-Spinning Reserve Calculation

The upward reserve requirement accounts for the largest, unexpected generation outage and the combined uncertainty in load, wind, and solar forecasts. Mathematically, the reserve need is expressed as in eq.(4).

$$RR_{N\ spin,upward} = P_{max,thermo} + 2.74 * \sigma_{Total} \quad (4)$$

Where:

- $P_{max,thermo}$  is the highest binding injection program value for a thermoelectric power plant, including its upward reserved capacity.
- $\sigma_{Total}$  is the total standard deviation.
- The factor 2.74 corresponds to a 99.7% confidence interval, ensuring robustness in reserve planning.

$P_{max,thermo}$  for 2023 & 2030 are 2000 MW [16] & 881 MW [17] respectively based on our elaboration on the largest power plants in Italian power plant portfolio.

### 2.3.2 Downward Non-Spinning Reserve Calculation

The downward reserve requirement is derived similarly, considering the largest hydroelectric pumping plant outage along with forecast errors in load and renewable generation, as in eq.(5).

$$RR_{N\ spin,downward} = P_{max,pumped\ hydro} + 2.74 * \sigma_{Total} \quad (5)$$

Where:

- $P_{max,pumped\ hydro}$  represents the maximum withdrawal program of a hydroelectric pumping plant, including its downward reserved capacity.
- The forecast error contributions are identical to the upward reserve calculation.

$P_{max,pumped\ hydro}$  for 2023 & 2030 are 1065 MW [18] & 1184 MW [19] respectively based on our elaboration on the largest power plants in Italian power plant portfolio.

To accurately determine the total standard deviation of forecast errors ( $\sigma_{Total}$ ) two distinct methods were employed: the convolution method and the formula-based method. Both approaches aim to quantify the aggregated uncertainty arising from load, wind, and solar forecast errors, ensuring a robust estimation of non-spinning reserve requirements.

### 2.3.3 Convolution Method Calculation

Convolution is a mathematical technique used in probability theory to combine multiple independent random variables into a single probability distribution. In the context of reserve estimation, it is used to combine the forecast error distributions of load, wind, and solar generation. This results in a total uncertainty profile that better reflects how different sources of variability interact. Compared to direct summation methods, convolution provides a more accurate representation of system-wide uncertainty, especially when multiple sources of error overlap in time.

#### 2.3.3.1 Mathematical Formulation of Convolution

For two independent random variables  $X$  and  $Y$  with probability density functions (PDFs)  $f_X(x)$  and  $f_Y(y)$ , the convolution  $Z=X+Y$  is defined in eq.(6).

$$f_Z(z) = \int_{-\infty}^{\infty} f_X(x)f_Y(z-x)dx \quad (6)$$

This integral determines how the uncertainties of two distributions combine to form a new probability distribution. In our case, if  $X$  represents wind forecast error and  $Y$  represents solar forecast error, their convolution produces the total renewable generation uncertainty.

#### 2.3.3.2 Application of Convolution in Reserve Estimation

The convolution process in reserve estimation consists of three main steps, sequentially combining forecast errors to derive the total system uncertainty.

1. Extract individual forecast errors: forecast errors for Load ( $E_{LOAD}$ ), Solar ( $E_{SOLAR}$ ) and Wind ( $E_{WIND}$ ) are obtained from historical data. Each forecast error is assumed to follow a normal distribution (Figure 2), characterized by its mean and standard deviation, as expressed in eq.(7), eq.(8) and eq.(9).

$$E_{LOAD} \sim \mathcal{N}(\mu_{LOAD}, \sigma_{LOAD}^2) \quad (7)$$

$$E_{SOLAR} \sim \mathcal{N}(\mu_{SOLAR}, \sigma_{SOLAR}^2) \quad (8)$$

$$E_{WIND} \sim \mathcal{N}(\mu_{WIND}, \sigma_{WIND}^2) \quad (9)$$

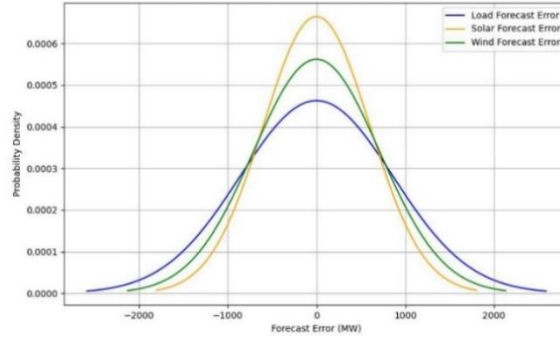


Figure 2. Normal Distribution of Forecast errors

2. First Convolution combining Wind & Solar uncertainties: since wind and solar power generation contribute jointly to renewable variability, their uncertainties must be combined first. The probability of distribution of the total renewable uncertainty is obtained through the convolution of their respective PDFs (Figure 3), following eq.(10).

$$f_{REN}(z) = \int_{-\infty}^{\infty} f_{SOLAR}(x) f_{WIND}(z - x) dx \quad (10)$$

Given that both errors follow a normal distribution, their convolution results in a new normally distributed uncertainty, defined as in eq.(11).

$$\sigma_{REN}^2 = \sigma_{SOLAR}^2 + \sigma_{WIND}^2 \quad (11)$$

While the mean value remains the sum of individual means, according to eq.(12).

$$\mu_{REN} = \mu_{SOLAR} + \mu_{WIND} \quad (12)$$

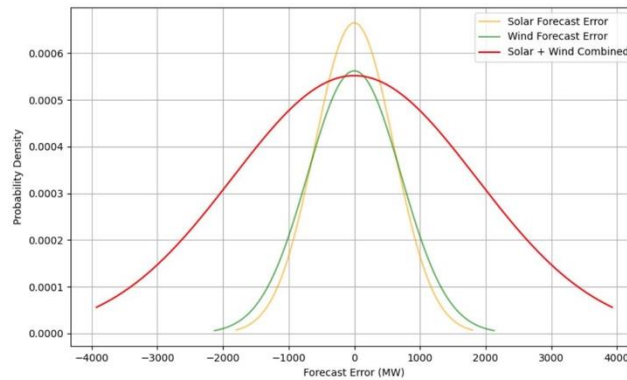


Figure 3. First Convolution combining Wind & Solar uncertainties

3. Second Convolution combining Renewable & Load uncertainties: the next step involves combining the total renewable uncertainty distribution  $E_{REN}$  with the load forecast error  $E_{LOAD}$  using the convolution defined in eq.(13).

$$f_{TOTAL}(z) = \int_{-\infty}^{\infty} f_{LOAD}(x) f_{REN}(z - x) dx \quad (13)$$

Since both distributions are normally distributed, the result is another normal distribution, shown in Figure 4, with mean value and standard deviation following eq.(14) and eq.(15).

$$\sigma_{TOTAL}^2 = \sigma_{LOAD}^2 + \sigma_{REN}^2 \quad (14)$$

$$\mu_{TOTAL} = \mu_{LOAD} + \mu_{REN} \quad (15)$$

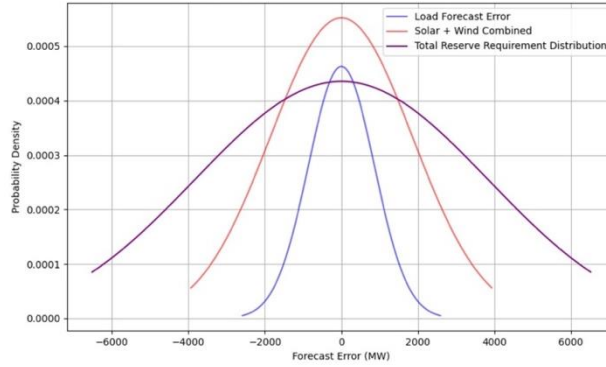


Figure 4. Second Convolution combining Renewable & Load uncertainties

4. Extract Standard Deviation and Compute Reserve Needs: The standard deviation ( $\sigma_{TOTAL}$ ) of this final distribution represents the system's total uncertainty, which is used to determine the non-spinning reserve requirement. The reserve is estimated using eq.(16), with a confidence multiplier based on a 99.7% probability interval:

$$RR_{Nspin} = 2.74 \cdot \sigma_{TOTAL} \quad (16)$$

#### 2.3.4 Empirical (Formula-based) Method Calculation

The formula-based method provides an analytical approach to estimating the total standard deviation of forecast errors, which is crucial for determining non-spinning reserve requirements. Unlike the convolution method, which integrates probability distributions, this approach directly computes the aggregated uncertainty by incorporating forecast errors from load, wind, and solar generation while accounting for their correlation.

##### 2.3.4.1 Mathematical Formulation

The total standard deviation of forecast errors is calculated using eq.(17).

$$\sigma_{total} = \sqrt{\sigma_{load}^2 + \sigma_{solar}^2 + \sigma_{wind}^2 + 2\rho \cdot \sigma_{load} \cdot \sqrt{\sigma_{solar}^2 + \sigma_{wind}^2}} \quad (17)$$

where:

- $\sigma_{total}$  = Total standard deviation of forecast errors
- $\sigma_{load}$  = Standard deviation of load forecast error
- $\sigma_{solar}$  = Standard deviation of solar generation forecast error
- $\sigma_{wind}$  = Standard deviation of wind generation forecast error
- $\rho$  = Correlation coefficient between load and renewable forecast errors

The correlation coefficient  $\rho$  is obtained using Pearson correlation analysis of historical load and renewable forecast errors. Based on this analysis,  $\rho$  is taken as:

- 0.05 for 2023
- 0.025 for 2030

These values reflect the observed relationship between load and renewable forecast errors in both years, with a lower correlation in 2030 due to changes in system behavior as renewable integration increases.

#### 2.3.4.2 Application in Reserve Estimation

1. Independent Forecast Error Contributions
  - a. The standard deviations of load, solar, and wind forecast errors are computed from historical data, capturing the variability in forecast accuracy for each component.
2. Correlation Adjustment
  - a. Since load forecast errors and renewable generation forecast errors are not entirely independent, a correlation coefficient ( $\rho$ ) is introduced.
  - b. The term  $2\rho \cdot \sigma_{load} \cdot \sqrt{\sigma_{solar}^2 + \sigma_{wind}^2}$  accounts for the interdependence between load and renewable fluctuations, ensuring that the estimated total uncertainty does not overestimate or underestimate the reserve requirement.
3. Final Reserve Estimation
  - a. The computed  $\sigma_{total}$  represents the aggregated system uncertainty in forecast errors.
  - b. The final non-spinning reserve requirement is determined by eq(18), where a confidence multiplier (e.g. 2.74 for a 99.7% probability) is applied.

$$RR_{Nspin} = 2.74 \cdot \sigma_{total} \quad (18)$$

Figure 5 illustrates the complete methodology for estimating reserve requirements based on forecasted and projected grid conditions. The process begins with the input data collection phase, which includes 2023 historical forecast data and 2030 projections for load and renewable generation, along with forecast error matrices derived from literature. The spinning reserves are calculated using standard formulations: aFRR is computed based on the maximum forecasted load using the ENTSO-E guideline, and mFRR is derived by scaling aFRR with the residual load ramp. For non-spinning tertiary reserves (both upward and downward) the reserve requirement is computed as the sum of a fixed capacity margin and a dynamic uncertainty term scaled by a confidence factor (2.74). This uncertainty ( $\sigma_{total}$ ) is evaluated through two distinct methodologies: the formula method and the convolution method. The formula method aggregates individual standard deviations for load, wind, and solar with a correlation term, while the convolution method integrates their probability distributions to derive the combined variance. Together, these steps define the hourly reserve needs required to maintain grid reliability under forecast uncertainty.

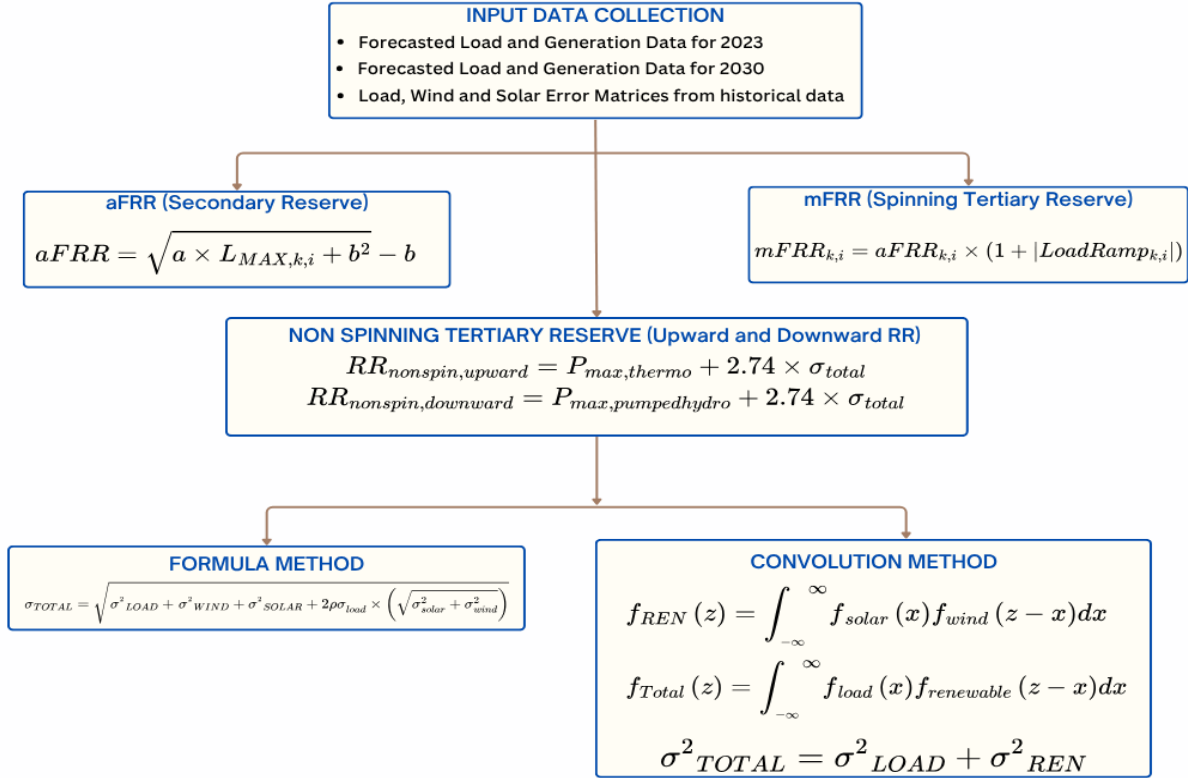


Figure 5. Reserve Estimation Methodology

## 2.4 Battery Energy Storage System Dispatch Model

To assess the potential contribution of energy storage to time-shifting and reserve requirements, a simplified BESS operation model was implemented for the year 2030. The battery system was defined with the following characteristics [20][7], aligned with future projections:

- Nominal power capacity: 8.33 GW
- Energy capacity: 50 GWh
- Round-trip efficiency: 96%
- Levelized Cost of Storage (LCOS): 50 €/MWh

The model uses an hourly market cost (MC) signal for the year 2030 to simulate time-shifting behavior [21]. For each 12-hour rolling window, the maximum, minimum, and average marginal costs are calculated. This 12-hour interval was chosen to reflect the typical intraday arbitrage cycle i.e., storing energy during low-cost periods and dispatching during high-cost periods, while accounting for operational constraints such as energy limits and cycle efficiency. Additionally, a shorter interval might miss full charge/discharge opportunities, while a longer interval could lead to unrealistic flattening of economic signals.

Within each 12-hour window, the spread (difference between maximum and minimum MC) is calculated as shown in eq.(19).

$$Spread = MC_{max} - MC_{min} \quad (19)$$

If the spread exceeds the LCOS (50 €/MWh), the battery is allowed to operate; otherwise, it is considered not economically viable for time-shifting routine in that 12-hour interval.

Within eligible windows, the model determines charging or discharging hours by comparing each hourly market cost to a profitability threshold, defined as in eq.(20).

$$Threshold = MC_{avg} + \frac{LCOS}{2} \quad (20)$$

A dispatch flag is then assigned per hour based on profitability:

- Flag = 1: Discharge (market marginal cost > threshold)
- Flag = -1: Charge (market marginal cost < threshold)
- Flag = 0: Idle (within non-profitable range)

This threshold accounts for the average cost level and introduces a buffer (LCOS/2) to avoid marginal or non-profitable operation due to round-trip losses. If the market cost in each hour exceeds the threshold, the battery is flagged to discharge (flag = 1). If the cost is lower than the threshold, the system is flagged to charge (flag = -1). If the market cost is within the range of  $\pm LCOS/2$  around the average, the system remains idle (flag = 0).

#### 2.4.1 SoC Evolution and BESS Dispatch Strategy

The SoC evolves dynamically based on charging and discharging decisions, starting from an initial SoC of 50% of the total energy capacity. The model ensures that SoC always stays within operational boundaries (0 to 50 GWh). For each hour  $t$ , the SoC is updated using eq.(21).

$$SoC_t = \min \left( E_{max}, \max \left( 0, SoC_{t-1} - \frac{P_{ch,req}}{\eta_{rtrp}} + P_{dis,req} * \eta_{rtrp} \right) \right) \quad (21)$$

Where:

- $E_{max}$  is Energy Capacity (50 GWh)
- $\eta_{rtrp}$  is the round-trip efficiency (0.96)
- $P_{ch,req}$  and  $P_{dis,req}$  are charging and discharging power requested, determined by eq.(22) and eq.(23).

$$P_{ch,req} = \min(0, Flag) * P_{nom} \quad (22)$$

$$P_{dis,req} = -\max(0, Flag) * P_{nom} \quad (23)$$

Where:

- $P_{nom}$  is nominal power (8.33 GW)

After computing the new SoC, the actual charging/discharging power values are calculated from the change in SoC, as described by eq.(24) and eq.(25).

$$P_{ch,real} = \max \left( 0, \frac{SoC_t - SoC_{t-1}}{\eta} \right) \quad (24)$$

$$P_{dis,real} = -\min(0, (SoC_t - SoC_{t-1})) * \eta \quad (25)$$

These real power values are then used in reserve contribution analysis to determine how much of the reserve requirement (upward and downward) can be met by the BESS at any given hour. Importantly, the real values may be lower than the requested power if SoC constraints prevent full operation.

Figure 6Figure 7 illustrate the dynamic interaction between electricity market prices, battery SoC, and real power dispatch across the year 2030. As shown, the SoC profile tends to remain high during

periods of low market prices, while it drops during high-price intervals indicating charging when electricity is cheap and discharging when it is profitable. Similarly, the power dispatch shows real charging behavior concentrated during low-price hours and discharging behavior aligning with peak price windows, confirming the market-based logic implemented in the dispatch algorithm. These plots qualitatively validate the core time-shifting strategy, where the battery system reacts to hourly MC signals to maximize arbitrage opportunities. Visually, the diagrams reflect the influence of the applied thresholds: the minimum, average, and maximum MC values can be inferred from the price trends, while the LCOS acts as the benchmark for dispatch decisions. This graphical representation supports the methodology and clarifies how the control strategy translates economic signals into operational behavior.

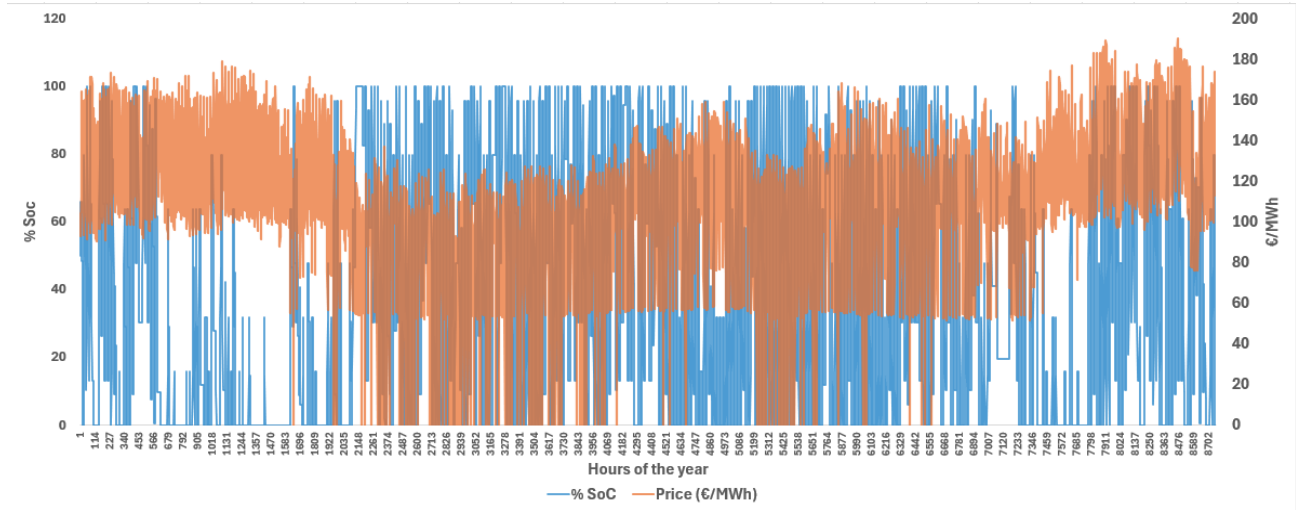


Figure 6. Percentage SoC BESS and electricity market prices for year 2030

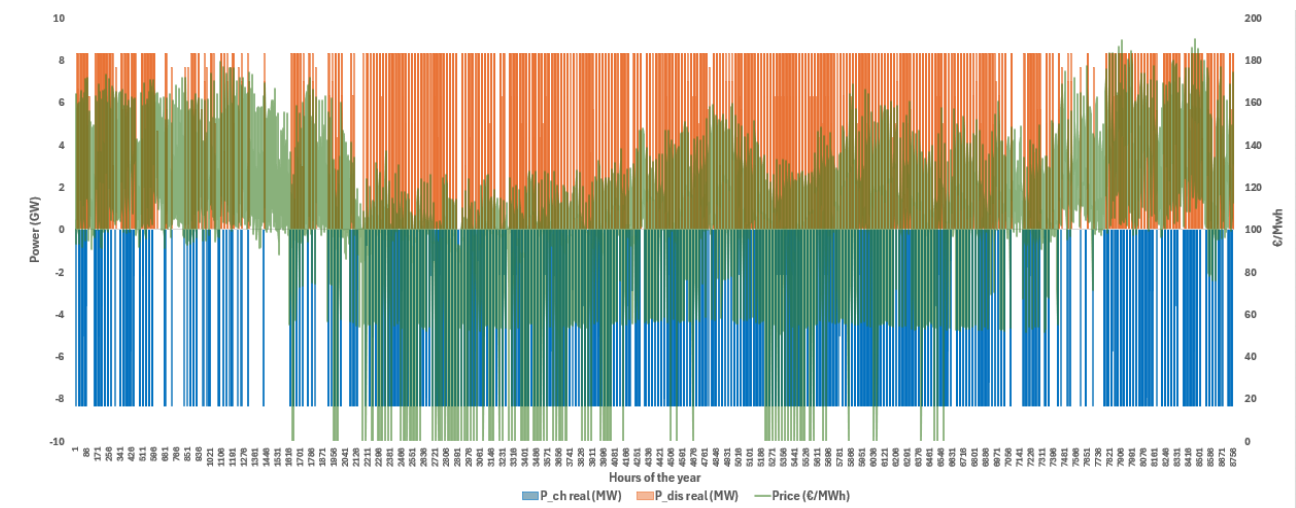


Figure 7. Real charging and discharging power of BESS and electricity market prices for year 2030

### 2.4.2 BESS Contribution to Reserve Requirement

To evaluate the ability of the BESS to contribute to system reserves, a time-resolved analysis was conducted for each hour of the year 2030. The model determines the available upward and downward reserve capacity the BESS can provide based on its operating condition, power rating, and energy state at that specific hour.

**Scenario 1: Idle State (No Active Charging or Discharging):**

If the battery is not actively charging or discharging, the full rated power capacity  $P_{nom}$  is theoretically available for reserves, subject to energy availability. The upward and downward reserve contributions are constrained as follows:

- Upward Reserve (Discharging Capacity):

$$R_{up} = \begin{cases} P_{nom}, & \text{if } E_{nom} \cdot SoC \geq P_{nom} \\ E_{nom} \cdot SoC, & \text{if } E_{nom} \cdot SoC \leq P_{nom} \end{cases} \quad (26)$$

- Downward Reserve (Charging Capacity):

$$R_{down} = \begin{cases} -P_{nom}, & \text{if } E_{nom} \cdot (1 - SoC) \geq P_{nom} \\ -E_{nom} \cdot (1 - SoC), & \text{if } E_{nom} \cdot (1 - SoC) \leq P_{nom} \end{cases} \quad (27)$$

**Scenario 2: Discharging State ( $P_{dis} > 0$ )**

When the battery is already discharging, its upward reserve capability is reduced because part of the capacity is in use. The available upward and downward reserves are given by:

- Upward Reserve (Discharging Capacity):

$$R_{up} = \begin{cases} P_{nom} - P_{dis}, & \text{if } E_{nom} \cdot SoC \geq (P_{nom} - P_{dis}) \\ E_{nom} \cdot SoC, & \text{if } E_{nom} \cdot SoC \leq (P_{nom} - P_{dis}) \end{cases} \quad (28)$$

- Downward Reserve (Charging Capacity):

$$R_{down} = \begin{cases} -(P_{nom} + P_{dis}), & \text{if } E_{nom} \cdot (1 - SoC) \geq P_{nom} \\ -E_{nom} \cdot (1 - SoC) - P_{dis}, & \text{if } E_{nom} \cdot (1 - SoC) \leq P_{nom} \end{cases} \quad (29)$$

This ensures that the battery does not overcharge while switching from discharge to charge under downward reserve activation.

**Scenario 3: Charging State ( $P_{ch} < 0$ )**

If the battery is actively charging, its upward reserve potential is enhanced because it can quickly reduce or stop charging to deliver power to the grid. The downward reserve, however, is limited by how much more the battery can still charge.

- Upward Reserve (Discharging Capacity):

$$R_{up} = \begin{cases} P_{nom} - P_{ch}, & \text{if } E_{nom} \cdot SoC \geq P_{nom} \\ E_{nom} \cdot SoC - P_{ch}, & \text{if } E_{nom} \cdot SoC \leq P_{nom} \end{cases} \quad (30)$$

- Downward Reserve (Charging Capacity):

$$R_{down} = \begin{cases} -(P_{nom} + P_{ch}), & \text{if } E_{nom} \cdot (1 - SoC) \geq P_{nom} + P_{ch} \\ -E_{nom} \cdot (1 - SoC) - P_{ch}, & \text{if } E_{nom} \cdot (1 - SoC) \leq P_{nom} + P_{ch} \end{cases} \quad (31)$$

In all scenarios, the SoC is updated dynamically using the actual charging and discharging profiles of the BESS. The calculated reserve contributions are constrained to respect both the instantaneous power limits and the available energy in the system. These values are then matched against the system reserve requirements at each hour to determine the effective reserve capacity that the BESS can provide, both in upward and downward directions.

Figure 8 presents the overall modeling framework used to estimate the contribution of BESS to time-shifting and system reserves in 2030, incorporating both technical constraints and market-based dispatch logic. The process begins with key input parameters, such as nominal power, energy capacity, round-trip efficiency, levelized cost of storage (LCOS), and hourly market prices.

In line with long-term MACSE contracts introduced in Italy [22], the BESS is primarily modeled as a time-shifting asset, its core function is to reduce price volatility by strategically charging and discharging based on market signals. This is implemented through a two-stage feasibility check: a 12-hour price spread is used to assess the overall profitability ( $\text{Spread} > \text{LCOS}$ ), and an hourly threshold logic determines whether to charge, discharge, or remain idle.

This price-based dispatch directly governs the SoC evolution of the BESS fleet, forming the operational baseline for reserve participation. SoC evolution and power dispatch are computed through a set of equations that incorporate physical constraints, including energy and power limits, as well as round-trip efficiency losses. Based on this SoC profile, the system evaluates available upward and downward reserve margins under three operating scenarios (idle, discharging, charging), as described in Sections 2.4.1 and 2.4.2 of the methodology. This structure ensures that reserve estimates are tied to realistic battery behavior shaped by economic feasibility and market-aligned operation.

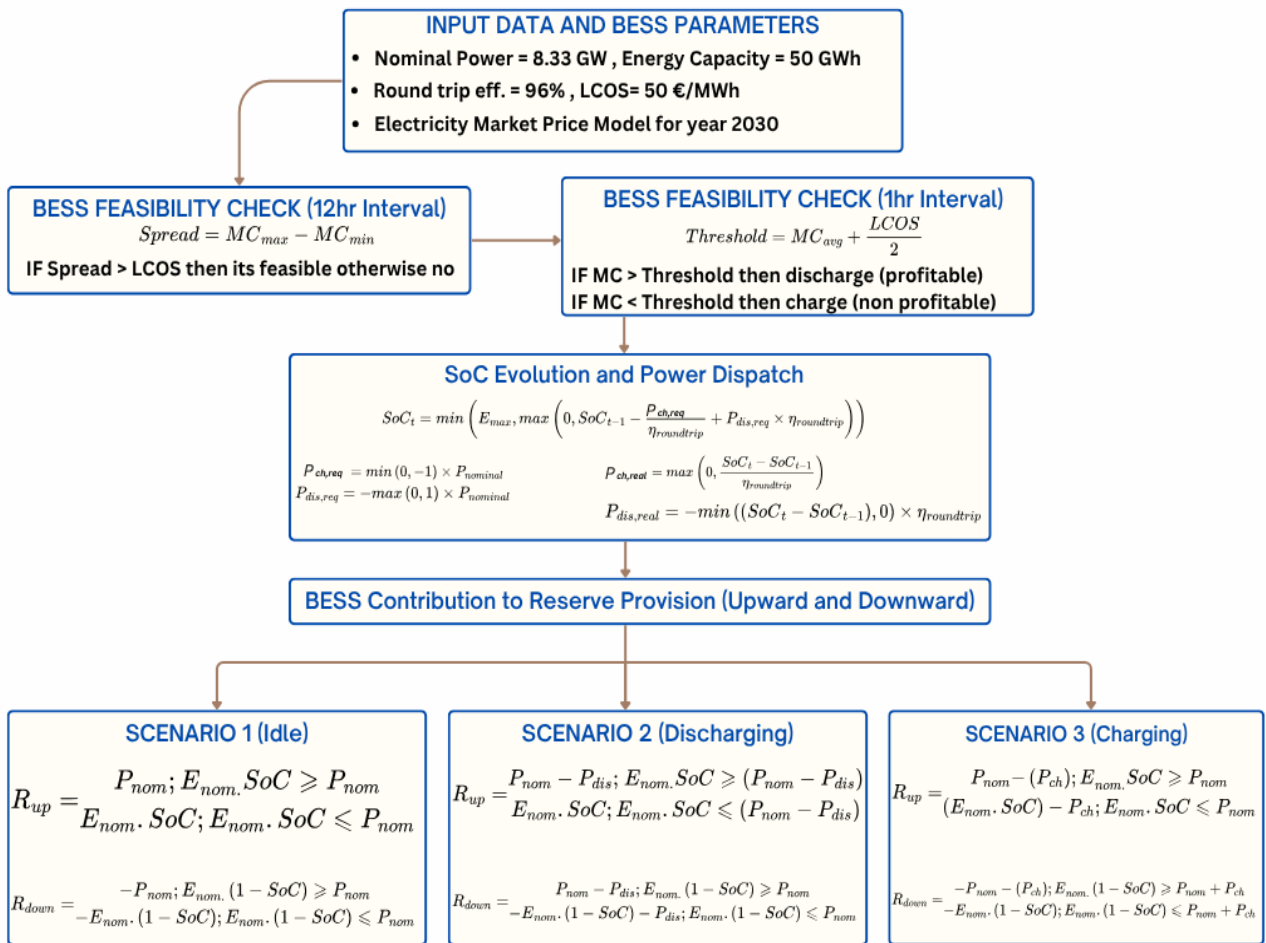


Figure 8. BESS Dispatch Model

### 3. Data Acquisition, Processing and Projection

Accurate reserve estimation and planning require a robust dataset that reflects current electricity demand and generation trends while incorporating future projections. This chapter outlines the data acquisition process, methodological steps taken to synchronize data from different sources, and the approach used to project electricity demand and renewable generation for 2030.

### 3.1 Formulation of Error Matrices

To estimate reserve requirements in a forward-looking manner, this study uses forecast error matrices for load, wind, and solar generation. These matrices represent the expected percentage error as a function of the forecasted value and were derived from historical data presented in Bovera et al. [5]. The paper provides graphical distributions of relative forecast errors across different operating conditions based on data from 2017 to 2019.

The forecast error matrices were constructed by considering as reference the statistical distribution of forecast errors derived from historical data from 2017 to 2019. The data was organized into structured matrices to enable time-resolved application across different operating conditions.

As shown in Table 1, the load forecast error matrix provides percentage error values indexed by day of the week and hour of the day. In the model, this matrix is used to assign an appropriate forecast error to each time step in the load forecast data. For each hourly timestamp, the corresponding error percentage is extracted from the matrix based on the weekday and hour. This value is then multiplied by the forecasted load to calculate the standard deviation of the load forecast error in megawatts. These error values are subsequently used in both the empirical and convolution-based methods to quantify the uncertainty component of the total reserve requirement.

Table 1. Load Error Matrix

Hours/Days	Monday	Tuesday	Wednesday	Thursday	Friday	Saturday	Sunday
0:00	2.69	2.80	2.64	2.48	1.97	2.19	3.02
1:00	2.69	2.77	2.60	2.08	1.93	2.29	3.20
2:00	2.69	2.72	2.59	2.07	1.92	2.47	3.28
3:00	2.69	2.66	2.60	2.05	1.93	2.66	3.46
4:00	2.69	2.60	2.65	2.00	1.98	2.83	3.38
5:00	2.69	2.51	2.12	1.96	2.07	3.06	3.20
6:00	2.69	2.44	2.12	1.94	2.23	3.09	3.02
7:00	2.69	2.40	2.05	1.93	2.48	3.02	2.84
8:00	2.69	2.49	1.97	1.96	2.67	2.95	2.71
9:00	2.69	2.42	1.90	2.03	2.73	2.87	2.65
10:00	2.69	2.30	1.86	2.17	2.89	2.81	2.65
11:00	2.69	2.20	1.84	2.40	2.84	2.76	2.13
12:00	2.69	2.13	1.88	2.62	2.75	2.74	1.60
13:00	2.63	2.09	1.96	2.55	2.66	2.74	1.08

14:00	2.55	2.08	2.16	2.49	2.60	2.78	0.56
15:00	2.49	2.09	2.41	2.44	2.59	2.31	0.56
16:00	2.45	2.15	2.46	2.40	2.64	2.28	0.56
17:00	2.43	2.31	2.52	2.38	2.75	2.27	0.56
18:00	2.44	2.55	2.53	2.37	2.45	2.27	0.57
19:00	2.48	2.67	2.51	2.37	2.15	2.28	0.57
20:00	2.56	2.75	2.49	2.39	2.10	2.34	0.56
21:00	2.72	2.77	2.46	2.44	2.07	2.43	0.56
22:00	2.87	2.73	2.46	2.07	2.09	2.56	0.56
23:00	2.85	2.69	2.46	2.02	2.13	2.73	0.56

The solar forecast error matrix, as shown in Table 2, was derived by taking as reference the statistical distribution curve presented in the literature which relates PV forecast uncertainty to the ratio between Forecasted PV output to the maximum installed PV capacity. For 2023, the installed PV capacity is taken as 30.3 GW. The installed capacity for 2030 is taken as 80GW [23].

Each row of the matrix corresponds to a forecast ratio and its associated error value, expressed as a fraction. In the model, for each hourly timestep, the forecasted PV output is divided by the installed PV capacity to determine the corresponding forecast ratio. Using this ratio, the model selects the appropriate error fraction from the matrix and multiplies it by the forecasted PV value. This gives the standard deviation ( $\sigma$ ) of the PV forecast error in megawatts for that timestep. This represents a cautious estimation approach, acknowledging that forecast errors in 2030 may be lower than historical values due to expected improvements in forecasting techniques.

Table 2. Solar Error Matrix

Forecast Ratio (PV / Max)	Forecast Error (%)	Forecast Error (Fraction)
0.025	1.5	0.015
0.075	3.8	0.038
0.125	6.1	0.061
0.175	7.2	0.072
0.225	8.1	0.081
0.275	9.5	0.095

0.325	10.0	0.111
0.375	10.5	0.105
0.425	11.0	0.111
0.475	11.5	0.115
0.525	13.0	0.130
0.575	14.5	0.145
0.625	16.0	0.160
0.675	17.5	0.175
0.725	18.5	0.185
0.775	19.5	0.195
0.825	21.0	0.211
0.875	22.0	0.222
0.925	22.5	0.225
0.975	18.0	0.188

The wind forecast error matrix, as shown in Table 3, was derived by taking as reference the statistical distribution curve presented in the literature, which relates forecast uncertainty to the ratio of forecasted wind generation to total installed wind capacity. This forecast ratio indirectly reflects wind intensity, which is strongly correlated with error variability. For the year 2023 and 2030 the installed wind capacity is taken as 12.34 GW [24] and 19 GW [25] respectively.

Each row in the matrix maps a specific forecast ratio to a corresponding forecast error, expressed both as a percentage and a decimal fraction. During reserve calculation, the forecasted wind output for each hourly timestamp is divided by the installed capacity to determine its forecast ratio. This ratio is then used to retrieve the matching forecast error fraction from the matrix.

The error fraction is multiplied by the forecasted wind value to compute the standard deviation ( $\sigma$ ) of the wind forecast error in megawatts.

Table 3. Wind Error Matrix

Forecast Ratio (Wind / Installed)	Forecast Error (%)	Forecast Error (Fraction)
0.025	0.6	0.006
0.075	1.7	0.017

0.125	2.6	0.026
0.175	3.2	0.032
0.225	3.8	0.038
0.275	4.3	0.043
0.325	4.6	0.046
0.375	5.1	0.051
0.425	4.8	0.048
0.475	5.4	0.054
0.525	5.8	0.058
0.575	5.3	0.053
0.625	6.2	0.062
0.675	4.5	0.045

### 3.2 Data Acquisition 2023

The initial step of this study involved obtaining load and generation data for the year 2023 from Terna [26]. However, the datasets had inconsistencies in their time resolutions. The load data was provided at 15-minute intervals, while the generation data was available at 1-hour intervals. To ensure uniformity, the generation data was interpolated to match the 15-minute resolution of the load data.

The analysis begins with the construction of the Load Duration Curve (LDC) for 2023, utilizing data obtained from Terna. LDC was generated by sorting the hourly load values in descending order, providing insight into the distribution of load levels over the year. This curve serves as a fundamental reference for understanding system demand patterns and reserve requirements.

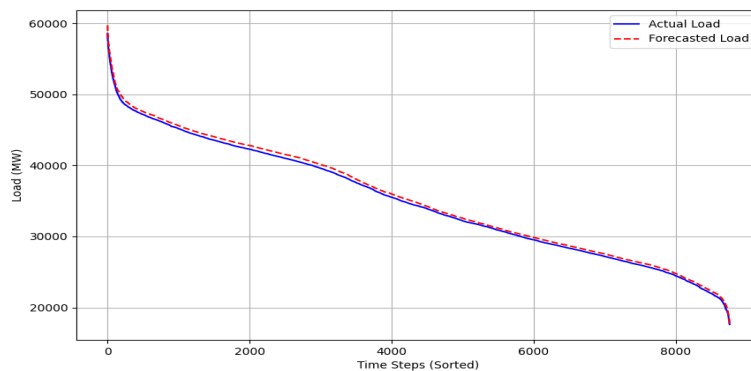


Figure 9. Load Duration Curve 2023

In Figure 9, the LDC for Terna 2023 compares actual and forecasted loads, demonstrating the accuracy of demand projections. The alignment between the two curves indicates the reliability of forecasting method.

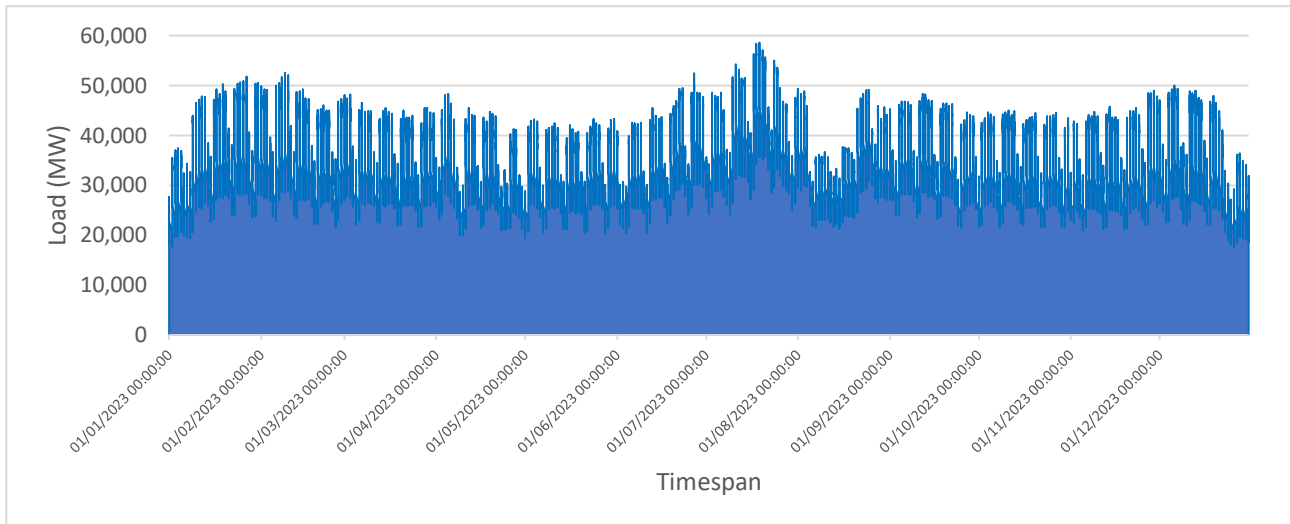


Figure 10. Load Hourly Profile for the year 2023

Load profile for 2023 exhibits significant daily and seasonal fluctuations, with frequent peaks exceeding 50,000 MW and a pronounced variability driven by weather-dependent consumption patterns as shown in Figure 10. The profile is characterized by higher intra-day volatility, reflecting demand shifts between daytime and nighttime as well as seasonal changes.

### 3.3 Projection of Electricity Demand, Renewable Generation and Market Price for 2030

To generate a forecasted demand profile for the year 2030, a bottom-up modeling approach was applied, producing an hourly dataset that spans the entire calendar year. This method allows for a detailed representation of seasonal changes, daily load patterns, and sector-specific electrification trends expected in a decarbonizing power system. The base demand data from 2023 was adjusted by incorporating additional demand components expected in 2030, including residential heating, representing increased adoption of electric heat pumps in households; cooling demand, primarily active during winter months; tertiary sector heating, covering commercial buildings, schools, hospitals etc.; industrial sector demand, accounting for the shift towards electrified industrial processes; and electric vehicle (EV) charging demand, based on forecasted uptake of EVs and their typical charging behavior [27]. Each of these components was modeled independently and added to the hourly baseline to obtain the total projected system load. Furthermore, the model incorporates behavioral adjustments for weekends and holidays. Lower electricity consumption is observed during non-working days, which was accounted for by applying a slightly reduced load profile. Specifically, the average demand during weekends is approximately 2% lower than on weekdays, aligning with typical reductions in commercial, industrial, and public sector activity.

This refined approach ensures that the resulting demand profile captures both structural energy transitions and operational characteristics of the Italian power system in 2030.

To account for efficiency improvements, the adjusted demand was scaled by 88.3%, aligning with the EU energy efficiency targets for 2030 [28]. This adjustment reflects the impact of more efficient electrical appliances and equipment.

For renewable energy generation, Italy's National Energy and Climate Plan (NECP) was consulted to determine the projected increase in installed capacity for wind and solar energy by 2030 [7]. According to NECP targets, wind energy capacity is expected to increase by a factor of 2.28, while solar energy capacity will increase by a factor of 2.61 compared to 2023 levels. To estimate the

forecasted renewable generation for 2030, the 2023 actual generation values were multiplied by these factors [29][30].

This methodology ensures a consistent and data-driven approach to projecting future electricity demand and renewable energy generation, aligning with Italy's 2030 NECP targets.

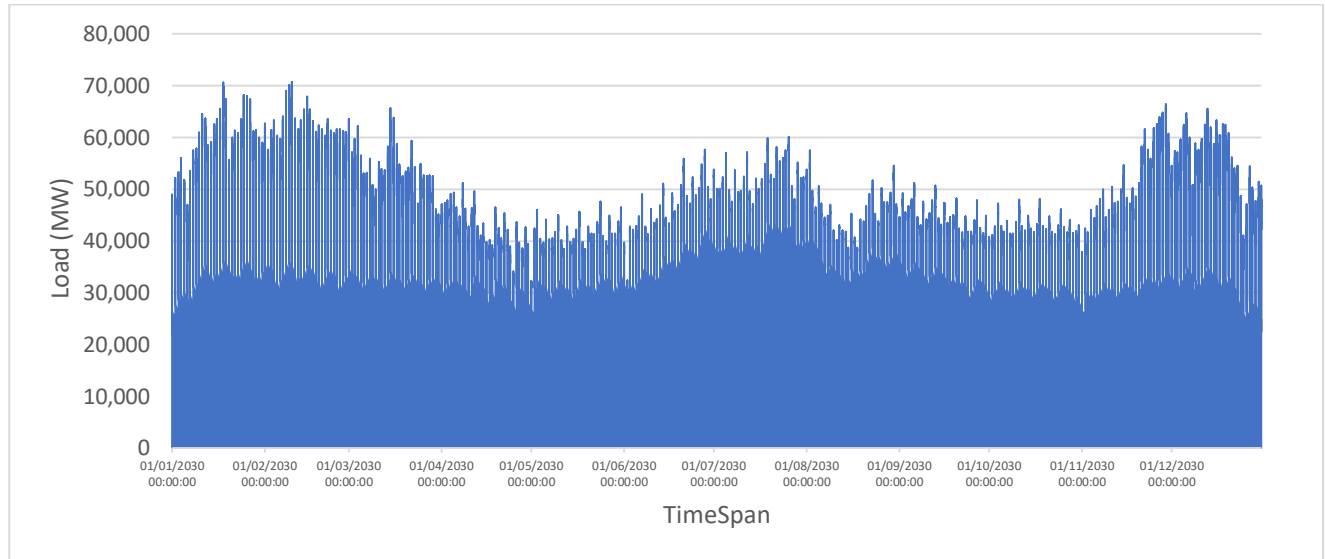


Figure 11. Forecasted Load Hourly Profile for the year 2030

In 2030, the forecast demand has increased significantly, with peaks approaching 70,000 MW due to higher electrification across residential, industrial, and transportation sectors, as shown in Figure 11. The winter peak is primarily driven by the electrification of heating, while summer demand has also risen, however to a lesser extent, due to the gradual electrification of cooling. Additionally, the increasing gap between workday and holiday demand reflects industrial consumption patterns, where higher loads on workdays are prominent as compared to the reduced activity on weekends.

Figure 12 presents the estimated hourly marginal cost (€/MW/h) for the Italian electricity market in 2030, the data was sourced from the literature [21] and processed to make a full year price profile. This price profile reflects the anticipated evolution of market conditions under high renewable energy penetration, capturing both typical daily variations and extreme events such as near-zero prices. The model is crucial for simulating BESS operation, as it determines when charging or discharging is economically feasible. It also forms the foundation for the time-shifting strategy, aligning BESS dispatch with hours of low-cost surplus and high-value scarcity.

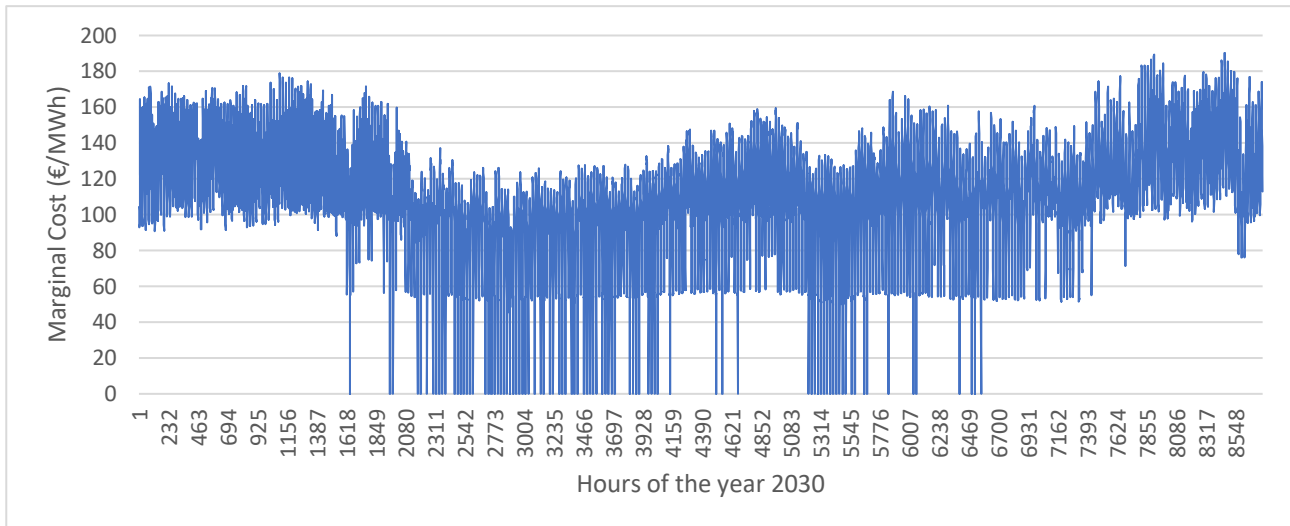


Figure 12. Market Price Estimation 2030

## 4. Results

This section presents the results of reserve requirement estimation for the Italian power system in the year 2030 and its comparison with year 2023, based on both formula-based and convolution-based methods. The analysis incorporates forecast uncertainties from load, solar, and wind generation, along with system ramping behavior and hourly demand fluctuations. Spinning and non-spinning reserve profiles are derived and examined across the full year to assess the impact of high renewable energy penetration and sectoral electrification. In addition, the operational behavior of the BESS is evaluated by first simulating its time-shifting strategy, which is computed as the baseline operating mode based on electricity market price signals and economic viability. Once the baseline SoC evolution and power profile is determined through this control logic, the BESS residual capacity is assessed for upward and downward reserve provision. This sequential approach reflects the practical prioritization of time-shifting as prescribed in Italian regulatory frameworks (MACSE) and ensures a realistic representation of role of the BESS. The resulting profiles offer critical insights into the adequacy, flexibility, and reliability of the future Italian grid under evolving energy scenarios.

### 4.1 Pearson Correlation Analysis

The Pearson correlation coefficient quantifies the linear relationship between forecast errors in load, solar, and wind generation. A coefficient close to zero indicates little to no correlation, while values approaching one or negative one indicates strong positive or negative relationships, respectively. The correlation results for 2023 and 2030 suggest weak dependencies among load, solar, and wind errors in both years as can be shown in Figure 13.

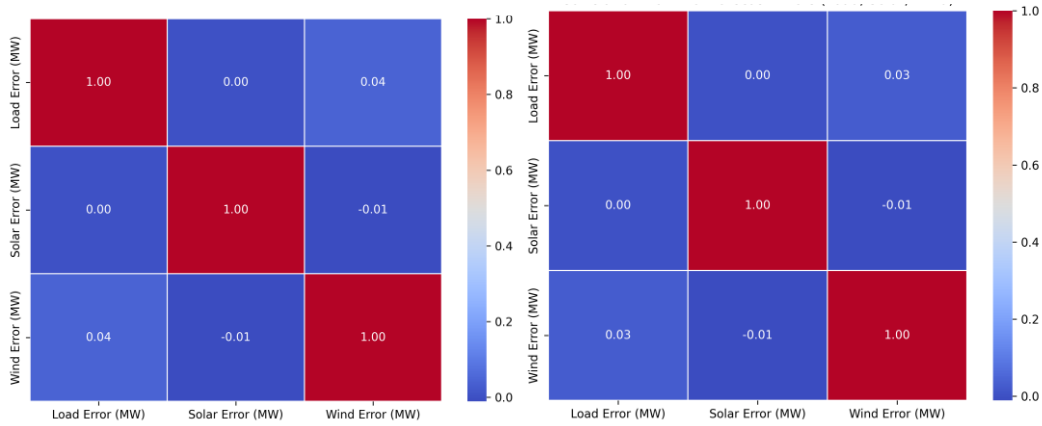


Figure 13. Pearson Correlation Matrix of forecast errors 2023(left) & 2030 (right)

The correlation between load and solar errors remains near zero (0.002 in 2023, 0.001 in 2030), indicating that solar forecasting inaccuracies have minimal impact on load errors. The correlation between load and wind errors decreases from 0.045 in 2023 to 0.025 in 2030, suggesting a reduced dependency, likely due to improved forecasting methods. The correlation between solar and wind errors remains nearly constant at -0.011, confirming their independent variability due to distinct meteorological influences. Beyond its application in tertiary non-spinning upward and downward reserve calculations via the empirical method, Pearson correlation was analyzed for both years to evaluate changes in forecasting relationships as renewable penetration increases. The reduced load-wind correlation in 2030 suggests that as wind capacity grows, its forecasting errors contribute less to overall load prediction errors, potentially due to advancements in forecasting models and energy balancing techniques. For further calculations, the selected correlation values of 0.05 for 2023 and 0.0251 for 2030 provide a more conservative estimate of forecast dependencies, ensuring accurate reserve estimations [31].

## 4.2 Reserve Estimation For 2023 and 2030

### 4.2.1 Automatic Frequency Restoration Reserve (aFRR) Estimation

The secondary reserve requirement, representing the automatic Frequency Restoration Reserve (aFRR), is shown for the years 2023 and 2030 in Figure 14.

In 2023, the aFRR profile shows a regular daily pattern with values typically between 350 MW and 650 MW, reflecting stable load dynamics and moderate renewable penetration. The smoother curve indicates limited forecast uncertainty and fewer abrupt load changes. In contrast, the 2030 profile is more irregular and elevated, with frequent peaks above 700 MW, especially in winter and late summer. This rise is driven by increased electrification (heating, EVs, industry) and higher shares of variable renewable energy, which introduce greater forecast volatility. Rapid net load ramps, particularly during sunrise and sunset, further amplify reserve needs, highlighting the growing impact of renewable integration on reserve requirements.

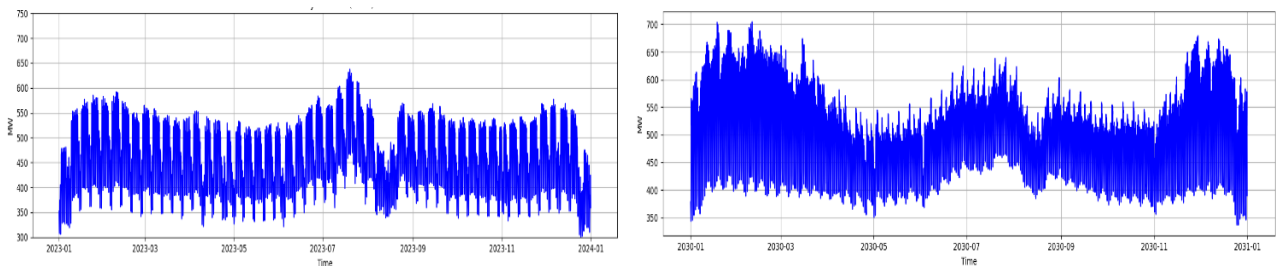


Figure 14. Secondary reserve requirement hourly profile 2023 (left) and 2030 (right)

Overall, the aFRR results demonstrate that by 2030, the Italian power system will not only require more secondary reserves on average but will also face more unpredictable and concentrated reserve demands. This underscores the need for increased system flexibility, improved forecasting accuracy, and fast-responding resources such as battery energy storage systems to maintain operational stability under high-renewable scenarios.

#### 4.2.2 Manual Frequency Restoration Reserve (mFRR) Estimation

The spinning reserve requirements, corresponding to the manual Frequency Restoration Reserve (mFRR), are shown for 2023 and 2030 in Figure 15. These values are derived by scaling the aFRR through a factor that reflects the relative ramping intensity of the residual load. Unlike aFRR, which responds to short-term frequency deviations, mFRR is designed to restore system balance over longer timeframes and is particularly sensitive to net load variability.

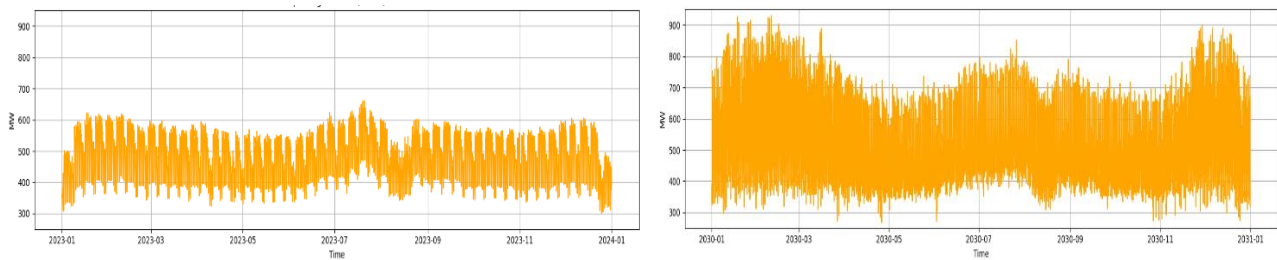


Figure 15. Spinning Tertiary reserve requirement profile 2023 (left) and 2030 (right)

The 2023 mFRR profile shows a consistent and structured pattern, with moderate fluctuations aligned with typical demand cycles. Ramp events are limited, reflecting stable system conditions. In contrast, the 2030 profile is more irregular and volatile, with frequent sharp spikes caused by rapid shifts in renewable output and electrified demand. Although the range remains similar, the higher frequency of sudden ramps indicates greater intra-hour variability. This growing volatility underscores the increasing importance of mFRR for grid stability, especially as aFRR alone may no longer be sufficient during fast transition periods.

#### 4.2.3 Non-Spinning Tertiary Reserve Estimation by Convolution Approach

The convolution method provides a probabilistic approach to estimating non-spinning tertiary reserves by integrating forecast error distributions. The results highlight a significant increase in both upward and downward reserve requirements from 2023 to 2030, driven by higher system-wide uncertainty and increased renewable penetration.

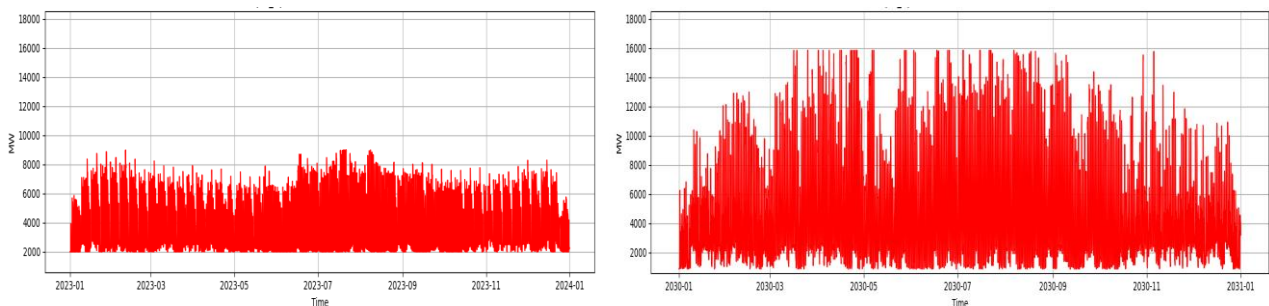


Figure 16. Non-Spinning Tertiary Upward Reserves (Left-2023 Right-2030)

As illustrated in Figure 16, In 2030, non-spinning upward reserve requirements frequently exceed 12,000 MW, compared to typical peaks of around 8,000 MW in 2023. The 2030 profile also shows sharper fluctuations and a higher density of extreme values, particularly between March and September. This rise reflects increased net load uncertainty due to higher renewable penetration and

sectoral electrification. Compared to 2023, the overall variability and peak reserve demand in 2030 are significantly amplified, underscoring the need for rapid response backup capacity. The observed drop to below 2000 MW in minimum upward reserves for 2030 is a direct outcome of the reduction in maximum generator's power. Although the same error matrices (for load, wind, and solar) are used for both 2023 and 2030, the input data differ significantly as 2030 features higher total demand, increased renewable generation, and different residual load dynamics. We calculate standard deviations by multiplying the percentage error from the error matrix with the forecasted value, so higher forecasts with relatively lower errors in some hours can result in narrower error bands. When these are convolved, the resulting PDF for net imbalance is tighter, especially in stable hours with low net variability thus this leads to lower 99.5th percentile values in certain hours.

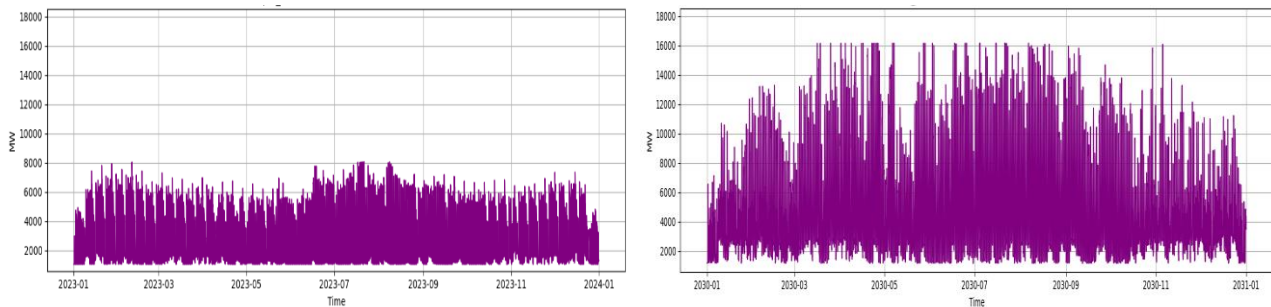


Figure 17. Non-Spinning Tertiary Downward Reserves (Left-2023 Right-2030)

Figure 17 presents the non-spinning downward reserve profile, showing a similar trend of reserve escalation. In 2030, non-spinning downward reserve requirements frequently reach values between 12,000 MW and 16,000 MW, compared to a typical range of 4,000–8,000 MW in 2023. The 2030 profile is marked by higher density and amplitude of reserve spikes, especially from March through October. This significant increase is linked to overgeneration risks during periods of high renewable output, particularly solar, requiring more capacity to absorb excess power. The contrast with 2023 highlights the growing need for flexible downward reserve capabilities in future grids.

#### 4.2.4 Non-Spinning Tertiary Reserve Estimation by Formula method

The formula-based estimation follows a deterministic approach, aggregating forecast errors directly rather than applying probabilistic distributions. Like the convolution-based results, the formula method also indicates a substantial rise in non-spinning upward reserve requirements in 2030 as shown in Figure 18. Reserve values frequently exceed 12,000 MW, with occasional peaks near 15,000 MW, compared to a more stable 2023 range of 4,000–8,000 MW. While the overall pattern is less spiky than the convolution output, the trend still reflects heightened variability in system conditions due to increased renewable integration and load uncertainty. The smoother curve in 2023 highlights the relative predictability of a less electrified system, while the 2030 profile points to a grid that must be equipped for faster and more frequent reserve activation.

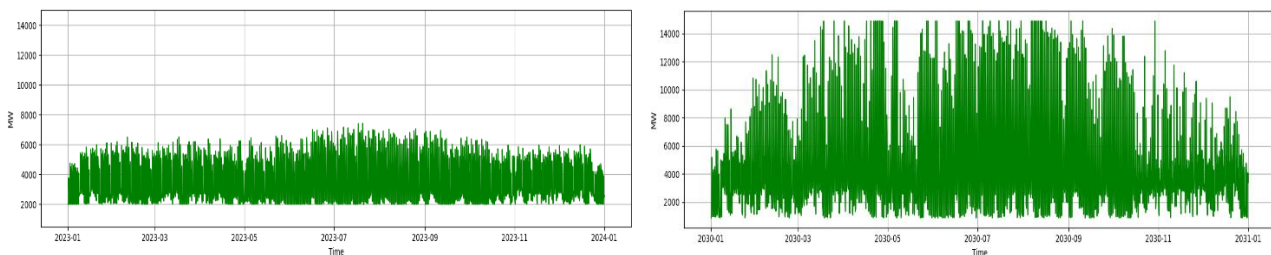


Figure 18. Non-Spinning Tertiary Upward Reserves (Left-2023 Right-2030)

The non-spinning tertiary downward reserve profiles for 2023 and 2030, computed using the formula-based method, show a significant rise in reserve requirements in 2030, reflecting increased renewable curtailment needs and system balancing challenges as shown in Figure 19.

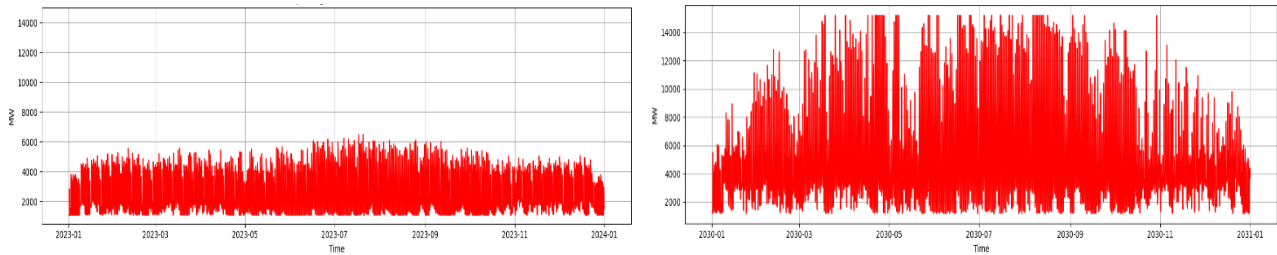


Figure 19. Non-Spinning Tertiary Downward Reserves (Left-2023 Right-2030)

The non-spinning tertiary downward reserve profiles for 2023 and 2030, computed using the formula-based method, show a significant rise in reserve requirements in 2030, reflecting increased renewable curtailment needs and system balancing challenges. In 2023, reserve requirements fluctuate between 1500 MW and 6000 MW, primarily driven by demand reductions and renewable overgeneration. By 2030, downward reserves exceed 14,000 MW, highlighting the amplified impact of higher renewable penetration and the need for enhanced flexibility in load management and energy storage.

The key differences between the two estimation methods highlight important trade-offs in reserve planning. Compared to the convolution method, the formula-based approach yields smoother reserve profiles with fewer extreme spikes, offering more stable and interpretable results for system planning. While the convolution method captures more detailed uncertainty by statistically combining forecast errors, it also tends to produce higher and more volatile reserve values, which may overestimate needs under certain assumptions. The formula method, aligned with ENTSO-E guidelines, provides a reliable and computationally efficient framework, making it more suitable for large-scale reserve analysis and scenario comparison

#### 4.2.5 Formula vs Convolution Method

The calculated results provide a quantitative comparison of non-spinning tertiary reserve requirements (upward and downward) for 2023 and 2030 using two methods: formula-based estimation and convolution-based estimation.

Table 4. Parameters Breakdown for 2023 and 2030

Parameters	2023 (MW) (Formula)	2023 (MW) (Convolution)	2030 (MW) (Formula)	2030 (MW) (Convolution)
Total Std.Dev ( $\sigma_{total}$ )	653.76	804.9	1455.07	1606.21
Reserve Requirement ( $2.74 \sigma_{total}$ )	1791.30	2205.42	3986.89	4401.01
RR Non-Spinning Upward	3791.30	4205.42	4867.9	5282.02
RR Non-Spinning Downward	2856.30	3270.42	5170.9	5585.01

The comparison between formula-based and convolution-based methods reveals key differences in how forecast uncertainty is handled in reserve estimation. As shown in Table 4, the convolution

method yields consistently higher values for total standard deviation ( $\sigma_{\text{total}}$ ) and resulting reserve requirements in both 2023 and 2030.

This outcome is expected, as the convolution method integrates the probability distributions of load, wind, and solar forecast errors. This probabilistic approach captures overlapping uncertainty more rigorously, often producing sharper spikes and broader distribution tails, as seen in the hourly reserve profiles. It reflects the full statistical range of possible deviations, especially under high renewable penetration scenarios like 2030, where the system experiences greater variability and ramping stress. However, the formula method remains highly practical and operationally relevant. It combines error components using a structured variance-based expression with a correlation term and provides transparent, scalable, and fast estimation suitable for system-level planning. In fact, despite its slightly lower reserve estimates, the formula method offers stable and interpretable results, making it ideal for regulatory compliance, sensitivity studies, and scenarios where computational simplicity is essential.

In conclusion, while the convolution method provides a detailed probabilistic insight and may highlight peak uncertainty, the formula method offers a balanced trade-off between accuracy and usability, supporting robust planning without significant computational overhead. Both approaches are valuable, but the choice depends on the intended application, with the formula method being particularly suitable for systematic reserve planning in future grids.

Figure 20, Figure 21, Figure 22 and Figure 23 illustrate a comparison between the hourly reserve availability and the actual imbalances in 2023, providing insight into whether the estimated reserves were overestimated or underestimated using both methods.

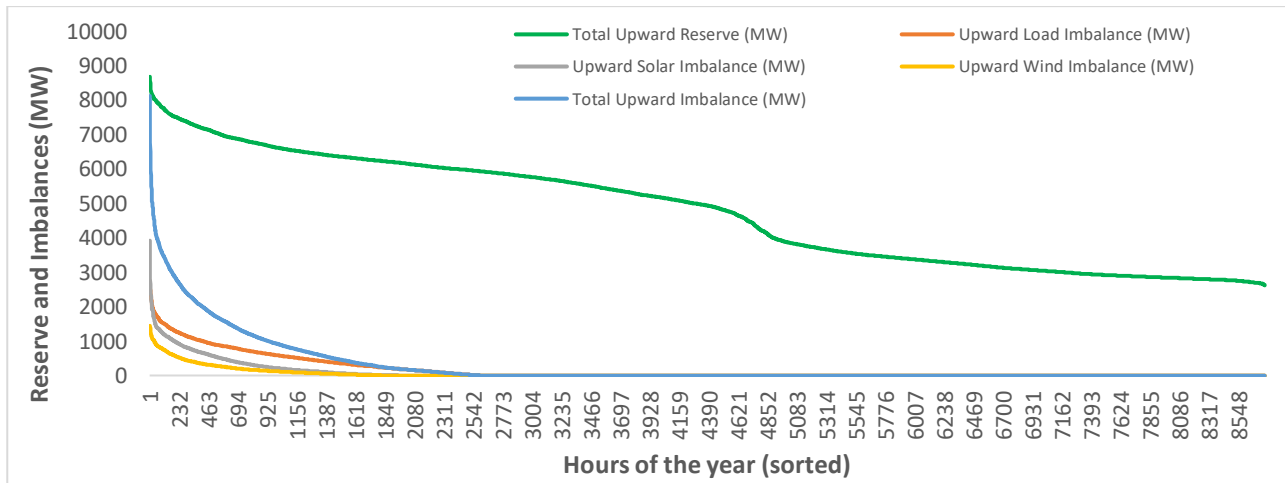


Figure 20. Comparison of Upward Reserves and Imbalances (Load, Renewable generation) – Formula Method 2023

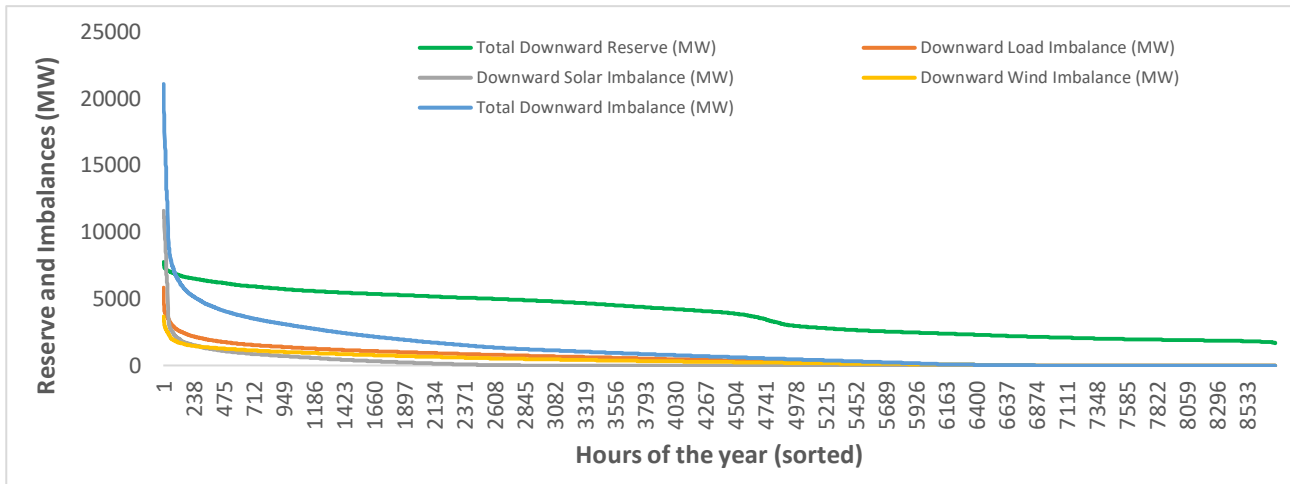


Figure 21. Comparison of Downward Reserves and Imbalances (Load, Renewable generation) – Formula Method 2023

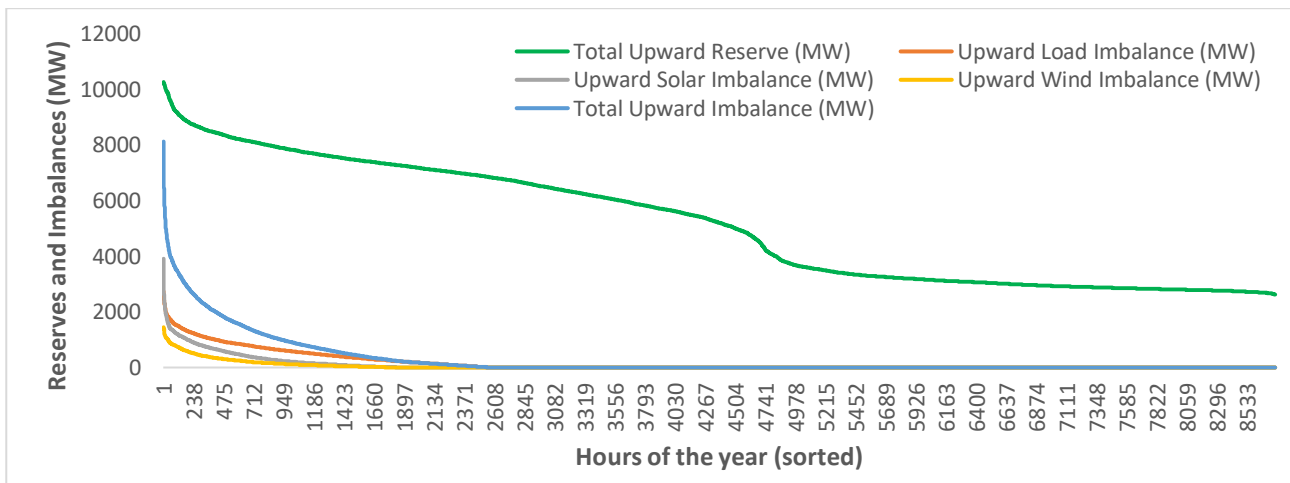


Figure 22. Comparison of Upward Reserves and Imbalances (Load, Renewable generation) – Convolution Method Method 2023

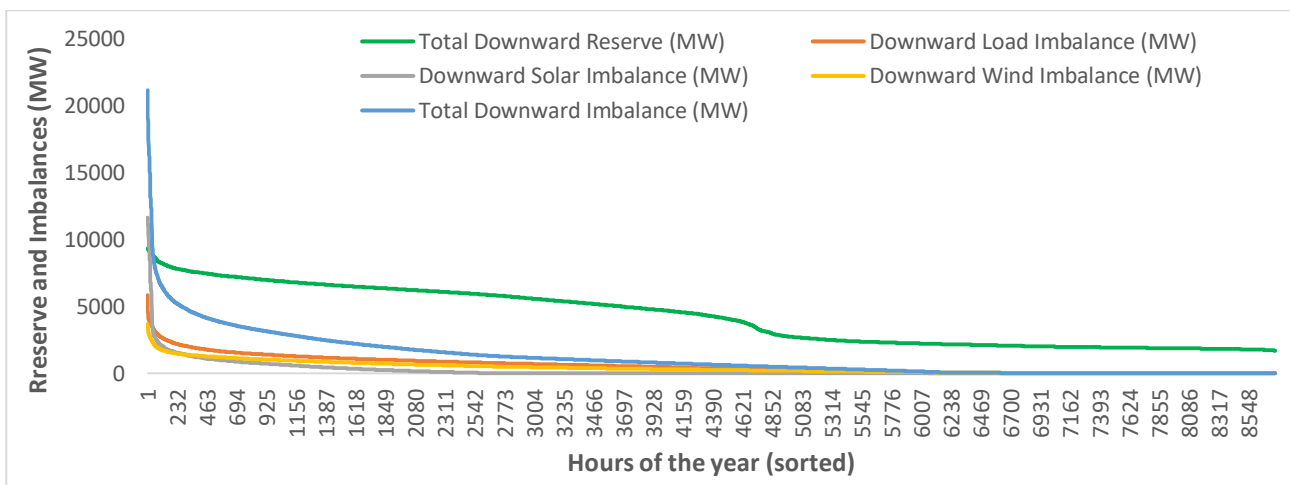


Figure 23. Comparison of Downward Reserves and Imbalances (Load, Renewable generation) – Convolution Method 2023

To perform this analysis, forecasted and actual values for load, solar, and wind were used to calculate hourly imbalances. Load imbalance was defined as actual minus forecasted load, where positive values indicate underestimation (requiring upward reserves) and negative values indicate overestimation (requiring downward reserves). For solar and wind, the imbalance was calculated as forecasted minus actual generation, since over-forecasting renewables results in a generation deficit (requiring upward reserves), while under-forecasting leads to surplus power (requiring downward reserves). These raw imbalance values were then separated into upward and downward components by extracting their positive and negative parts, respectively. The total upward and downward imbalances were obtained by summing the contributions from load, solar, and wind.

These were compared against the total upward and downward reserves, calculated as the sum of aFRR, mFRR, and non-spinning reserves (upward or downward depending on direction). By sorting and plotting all 8760 hours, these graphs provide a clear picture of whether the estimated reserves were sufficient to cover the real-time system needs, under both the formula-based and convolution-based approaches.

This analysis confirms that the upward reserve consistently exceeds the total upward imbalance across all 8760 hours, indicating that the system is well-prepared to handle unforeseen increases in net load. For the downward direction, the reserve margin is also sufficient in 8664 hours in formula method and 8713 hours in convolution method for a whole year as shown in Table 5. This suggests that both methods provide a conservative reserve allocation, especially in the upward direction, while maintaining near-complete coverage for downward imbalances as well.

Table 5. Reserve vs Imbalances Analysis

Key Parameters	2023 (No. of Hours) (Formula)	2023 (No. of Hours) (Convolution)
Total Upward Reserves > Total Upward Imbalances	8760	8760
Total downward reserves > Total Downward Imbalances	8664	8713

Despite this overall adequacy, the total downward imbalance is substantially higher than the upward imbalance, both in terms of peak values and cumulative energy content. This discrepancy arises primarily due to the dominant contribution of solar PV to downward imbalance. The system frequently encounters instances where solar generation is under-forecasted, leading to surplus generation during midday hours. When actual solar output exceeds forecasts, especially during high irradiance conditions, the grid experiences a supply surplus that must be mitigated by curtailing generation or increasing demand thus requiring downward reserves.

As Figure 20, Figure 21, Figure 22 and Figure 23 provided a clear and concise overview of whether the estimated reserves were sufficient to cover imbalances across the entire year, ranked from highest to lowest imbalance. However, the two additional hourly plots in Figure 24 and Figure 25 reveal the real-time dynamics of reserve deployment and imbalance behavior throughout the year. These graphs are valuable in visualizing temporal trends, sudden peaks, seasonal fluctuations, and the actual stress periods the system faces. Unlike the smooth view in sorted graphs, these time-series plots uncover the operational complexity and highlight specific instances of system strain.

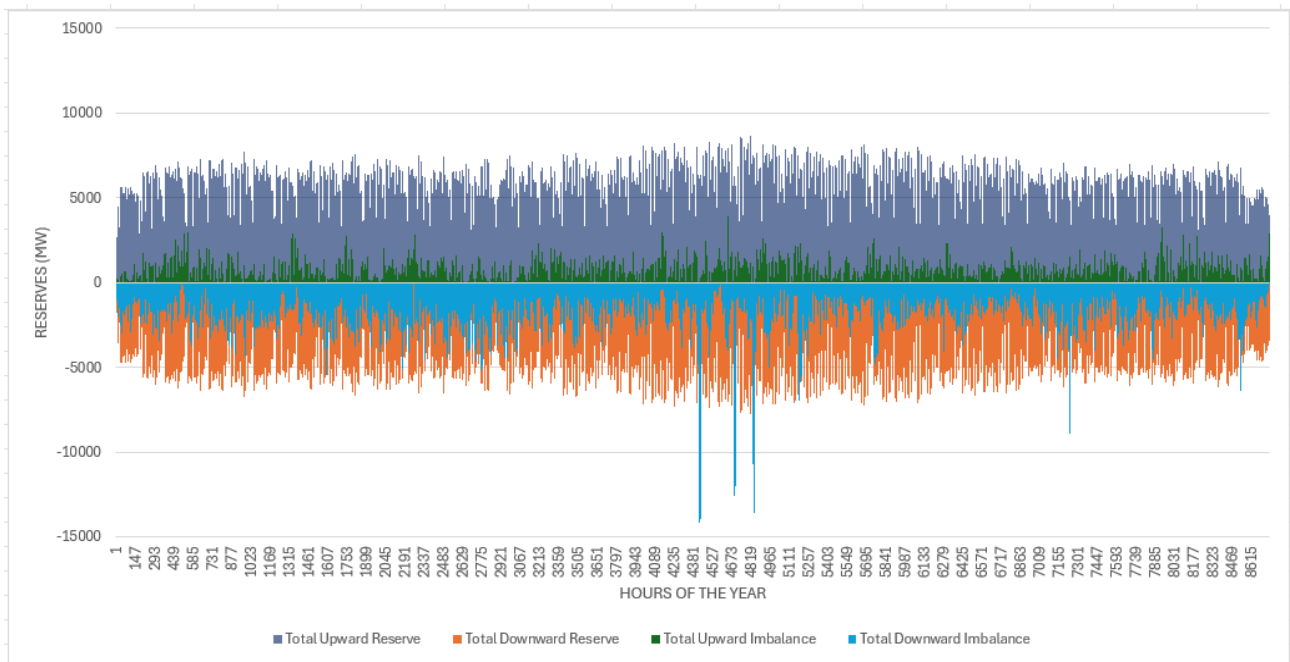


Figure 24. Imbalances vs Reserve Hourly Profile (Formula Method)-2023

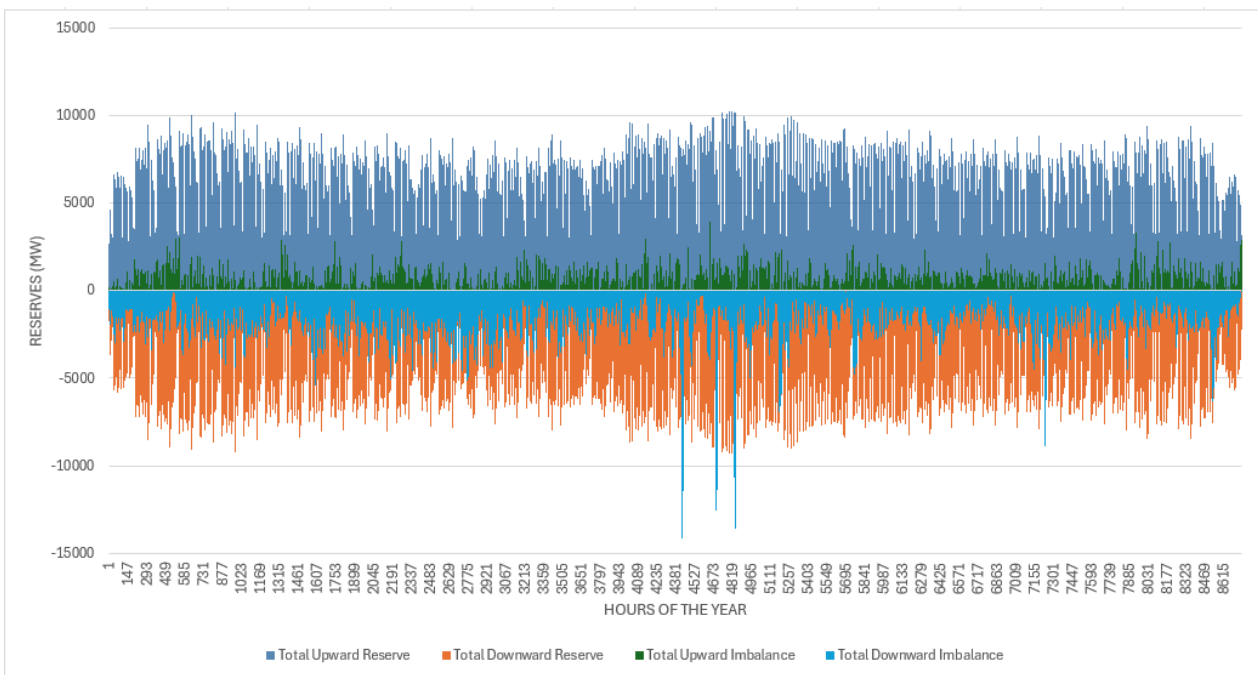


Figure 25. Imbalances vs Reserve Hourly Profile (Convolution Method) - 2023

From these graphs, several key observations emerge. Most notably, the total downward reserve requirement reaches extreme peaks exceeding 12,000 MW during the spring months (particularly April and May), aligning with periods of maximum solar generation and frequent over-forecasting events. These peaks coincide with midday hours when actual solar output surpasses forecasts, creating an excess supply that the system must curtail or absorb. The total upward reserve, although more stable, also exhibits sharp hourly spikes, especially in winter months like January and February, reflecting sudden demand surges combined with low-RES generation. Additionally, both plots show that downward imbalance events are more volatile and frequent, reinforcing earlier insights that managing overgeneration will be the principal challenge in a high-renewables grid scenario. These time-series visualizations are thus instrumental in supporting operational planning

and identifying critical hours that demand additional flexibility, curtailment, or market response mechanisms

### 4.3 BESS Dispatch and Contribution to Reserve Analysis

This section presents the operational results of the BESS for the year 2030, focusing on its dispatch behavior, time shifting, and contribution to system reserves. Key indicators such as the SoC, charging/discharging power, and reserve availability are analyzed on an hourly basis. The BESS operation was governed by a market-based dispatch logic, which first prioritizes renewable energy time shifting; charging during low-price hours and discharging during high-price periods; based on price spread and profitability thresholds relative to the LCOS. Once time-shifting opportunities are met, the BESS becomes available for upward and downward reserve provision. The aim is to assess how effectively the BESS can participate in both services while maintaining operational feasibility. The results provide insight into the flexibility of the system and the strategic value of battery deployment in a high-renewable energy scenario.

#### 4.3.1 RES Time Shifting

In this study, RES time shifting was implemented using a market-based dispatch strategy applied to the 2030 electricity price profile. A 12-hour price spread check was performed to determine the economic feasibility of storage operation, followed by an hourly threshold comparison to decide whether the BESS should charge or discharge. If the price spread exceeded the levelized cost of storage (LCOS), the battery was allowed to operate. The dispatch logic ensured charging during low-price hours and discharging when market prices exceeded a defined profitability threshold. Figure 26 illustrates the impact of this approach on the SoC profile of the battery over the year 2030.

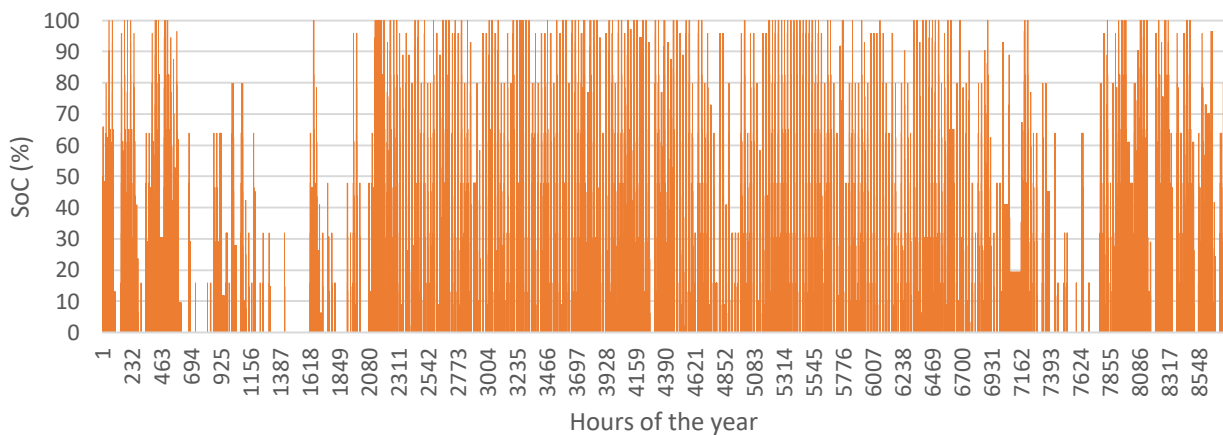


Figure 26. Percentage (%) SoC of BESS - 2030

The profile highlights the dynamic operation of the battery system in response to market signals, particularly electricity price fluctuations. The SoC varies between 0% and 100%, indicating frequent charge and discharge cycles throughout the year. The battery often remains partially charged rather than idle, demonstrating its active role in shifting renewable energy temporally. Periods of sustained high SoC typically correspond to low-price or surplus generation intervals, while rapid drops in SoC indicate discharging during high-price windows. The irregularity in SoC patterns reflects both seasonal variability and the economic feasibility filters applied (e.g., spread > LCOS and hourly threshold logic), which govern when the battery is allowed to operate.

Figure 27 illustrates the distribution of the battery SoC over the year, segmented into percentage ranges. It reveals that the BESS spent nearly 40% of its operational hours (3488 hours) at very low

charge levels (0–10%), indicating prolonged periods of depletion. This behavior is driven by the strict profitability conditions used in the RES time shifting strategy, where charging is avoided unless market conditions offer a spread greater than the LCOS. As a result, the system frequently discharges when marginal costs are high but remains underutilized during periods with insufficient economic incentive to recharge, leading to a skewed SoC distribution.

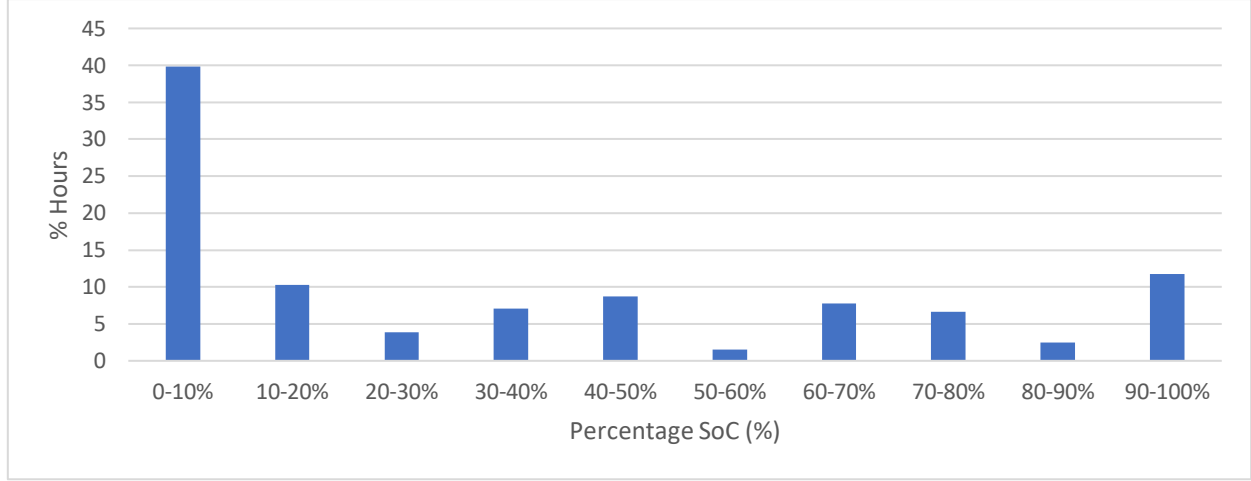


Figure 27. % SoC BESS & % Hours - 2030

To assess the effectiveness and operational behavior of the BESS, it is important to go beyond hourly power trends and analyze cumulative performance indicators. Metrics such as equivalent full cycles, energy throughput, and turnover index provide deeper insight into how intensively the BESS was utilized, how frequently it cycled, and how responsive it was under the applied control strategy.

The number of equivalent full cycles quantifies how often the battery has been fully charged and discharged over the year, regardless of whether this occurred in partial steps. In this case, the result of approximately 214 cycles indicates relatively active usage, consistent with a system responding to daily market price signals and providing reserve support when profitable.

The average daily energy throughput is calculated by eq.(32).

$$\text{Average Daily Throughput (MWh)} = \frac{\sum P_{\text{charge,real}} + P_{\text{discharge,real}}}{\text{days}} \quad (32)$$

We obtain nearly 61 GWh/day, which reflects the intensity of battery usage on a day-to-day basis. Given that the total energy capacity is 50 GWh, this result means that, on average, the battery exchanges more energy per day than its rated capacity, suggesting frequent partial cycling and strong participation in market-driven charging/discharging. It implies that the BESS is actively used, not idle, and is likely to capture multiple opportunities across the day (e.g. morning and evening peaks).

Moreover, high daily throughput is often associated with better economic performance, as it increases potential revenues, but it also implies higher degradation, so there is a trade-off between profit and lifetime. In this context, 61 GWh/day is a relatively high value, indicating an aggressive operational strategy that prioritizes maximizing value from arbitrage and reserve provision.

Finally, the turnover index (3 hours) represents the time it takes to fully charge or discharge the battery at nominal power. A low turnover index highlights the ability of BESS to rapidly respond to system needs, making it well-suited for high-frequency reserve provision and time-shifting applications. Together, these indicators provide valuable insight into the BESS operational stress, economic viability, and system-level impact.

Figure 28 & Figure 29 illustrate the real hourly charging and discharging behavior of the BESS throughout the year 2030. The charging power (shown as negative values) remains frequently at full capacity (around -8.33 GW), indicating that whenever the BESS is allowed to charge based on market conditions and SoC constraints, it utilizes its maximum power limit. On the other hand, the discharging profile shows more scattered but equally intensive operation, often discharging at or near full capacity. This reflects the BESS dynamic response to price signals, where profitable discharge windows are exploited fully.

The high frequency of full-power operations in both directions suggests that the BESS is being operated effectively to maximize arbitrage opportunities. Moreover, the temporal distribution of these events confirms that the system is highly responsive to intra-day price variability. These patterns support the earlier findings of a high turnover index and significant daily throughput, indicating that the battery is actively participating in market-driven time shifting.

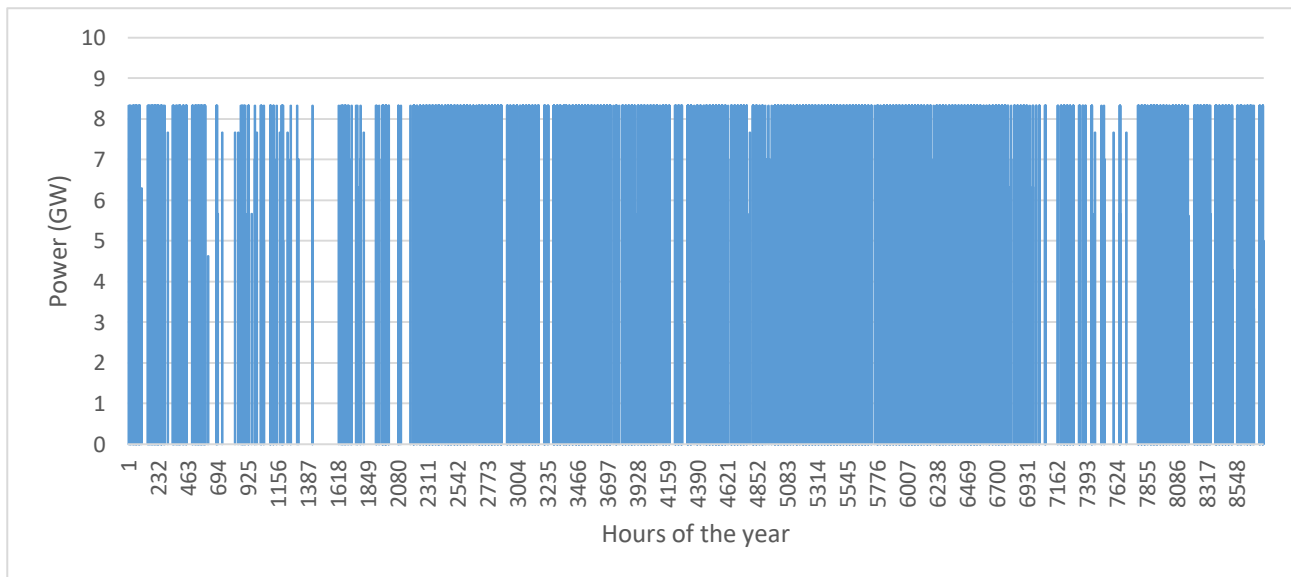


Figure 28. Real Discharging behavior by BESS 2030

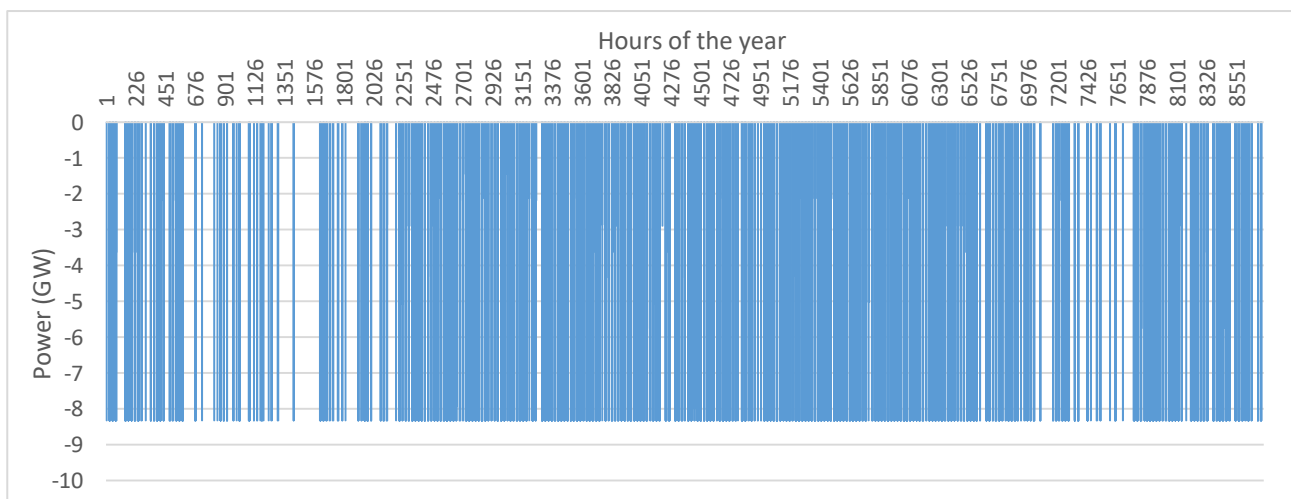


Figure 29. Real Charging behavior by BESS 2030

#### 4.3.2 BESS Contribution to Reserve Requirement

This section evaluates the ability of the BESS to support system reserve requirements, building upon its primary operation as a time-shifting asset. The hourly dispatch profile and SoC evolution, generated from the 2030 price-driven model serve as the baseline for reserve availability assessment.

The analysis distinguishes between upward and downward reserve contributions, while accounting for technical constraints such as nominal power, usable energy capacity, round-trip efficiency, and real-time SoC limits.

Figure 30 illustrates the hourly reserve profile over the course of the year 2030. It compares the total upward and downward reserve requirements of the system with the corresponding hourly availability of BESS for contribution in reserves. Visually, the BESS appears more available in downward reserve provision than in the upward, and this trend is consistent throughout the year. Notably, the density of the downward bars is higher and more continuous, especially during periods of high solar generation when curtailment risk is elevated and BESS is likely operating in charging mode.

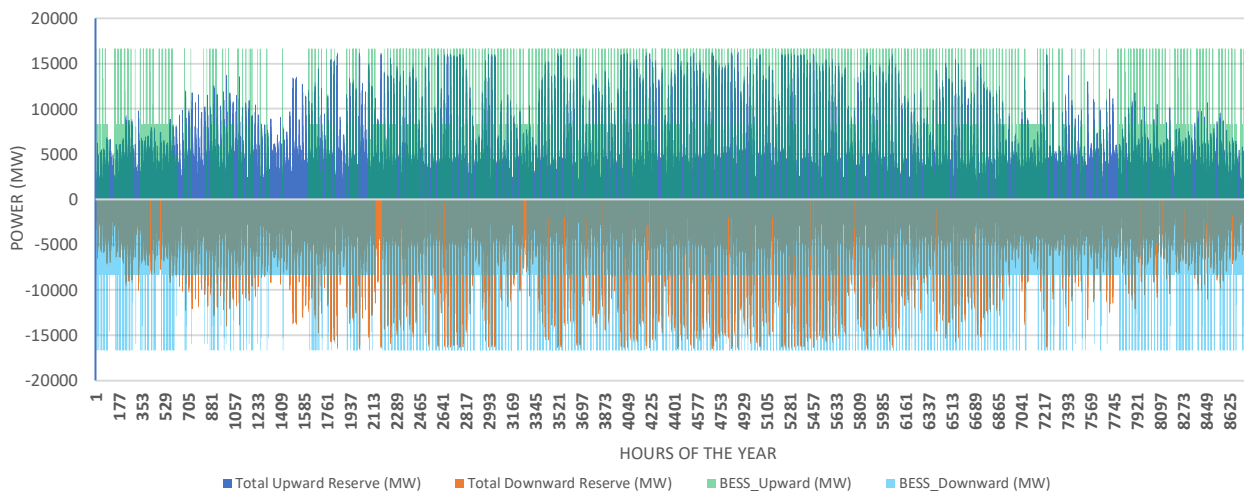


Figure 30. BESS availability and reserve requirement hourly profile - 2030

In particular, the BESS is consistently available for downward reserves across the year, with availability often approaching its technical limit. This reflects the BESS frequent charging behavior during low-price or surplus generation periods. In comparison, upward reserve availability appears more limited, constrained by SoC levels and prior discharge activity.

To quantify the BESS contribution, Table 5 below presents key metrics. Out of 8760 hours in the year, the BESS contributed to an upward reserve in 4397 hours (50%) and to downward reserve in 6890 hours (79%). However, mere contribution does not imply sufficiency. When we look at how often the BESS was able to fully satisfy the reserve requirement defined as meeting or exceeding the system reserve need in that hour, the numbers reduce understandably. The BESS satisfied the upward reserve in only 3495 hours (40%), while it satisfied the full downward requirement in 5930 hours (68%).

Table 6. Hourly BESS Contribution Analysis

Parameters	Hours	Percentage Hours (%)
BESS Contribution to Upward Reserves	4397	50%
BESS Full Satisfaction of Upward Reserves	3495	40%
BESS Contribution to Downward Reserves	6890	79%

BESS Full Satisfaction of Downward Reserves	5930	68%
---	------	-----

To gain a more understanding of the BESS effectiveness, Figure 31 presents a comparison between the actual system reserve requirement and the portion covered by the BESS, separately for both upward and downward directions. This visual allows us to move beyond raw availability and assess coverage; that is, how often and to what extent BESS is able to meet reserve demands.

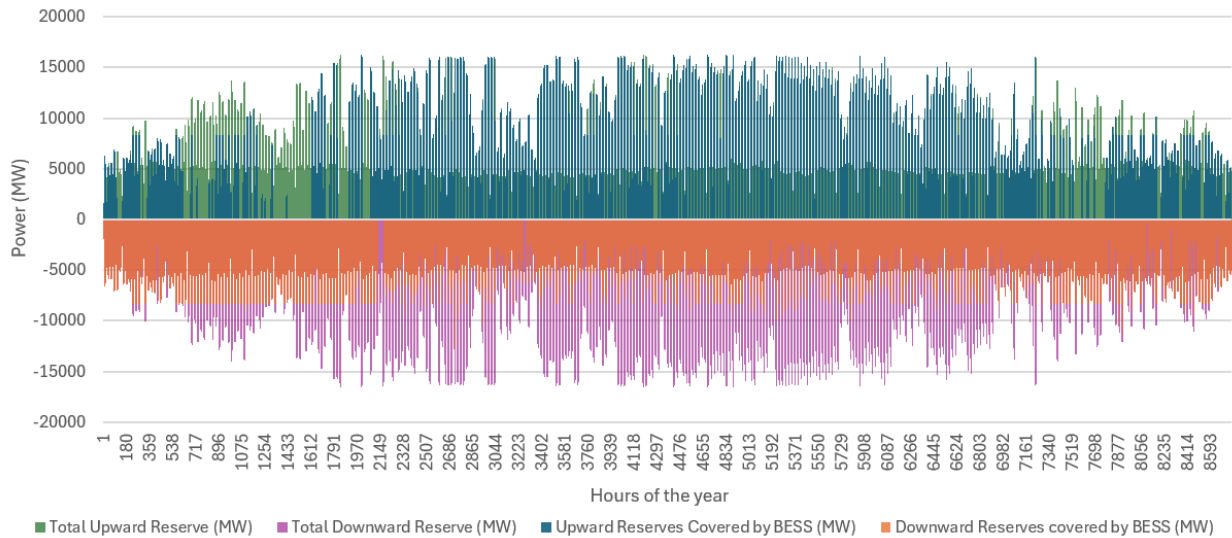


Figure 31. BESS Contribution to Upward and Downward Reserves - 2030

In this chart, each hour is split into two components for both upward and downward reserves: Upward Reserves Covered by BESS: the minimum between the required upward reserve and BESS availability. Upward Reserve not Covered by BESS: the residual gap when system need exceeds BESS availability. Downward Reserve Covered by BESS: the BESS availability when it is less than or equal to system requirement. Downward Reserve Not Covered by BESS: the excess requirement that BESS fails to meet. Compared to Figure 30 which visualized BESS availability, this representation explicitly isolates reserve shortfalls, thus making it much easier to evaluate coverage adequacy over time. It highlights moments where the BESS is underutilized due to system sufficiency (no coverage required), as well as periods where the storage system was insufficient despite full utilization particularly evident during high reserve events or SoC constraints.

The upward reserve not covered by BESS is the remaining part of the reserves that are not satisfied by BESS, and it appears consistently throughout the year, especially in the mid and early portions of the year. This suggests that the BESS regularly hits its discharge or SoC limits, unable to meet the upward reserve demand. Similarly, for downward reserves, the tallest spikes are also not fully met by the BESS, highlighting that during hours of extreme curtailment or excess generation, the battery alone is insufficient to absorb the full surplus. However, the overall density and spread of the downward reserves covered by BESS are higher than for the upward side. This supports the earlier numerical result that BESS satisfied around 68% of downward reserve needs, compared to only 40% for upward reserve needs. The relatively smoother and more continuous pattern of downward reserve coverage indicates the BESS is more active and effective in charging during surplus periods than discharging during shortages.

Both upward and downward unmet reserves spread out more prominently in the middle and start of the year, possibly aligning with summer and winter stress. In contrast, spring and autumn seem to show better reserve coverage. Overall, BESS actively contributes across most hours but rarely

fulfills the full requirement alone, especially for peak reserve needs. This reinforces its role as a partial, supportive asset rather than a complete replacement for conventional reserves.

It is important to emphasize that the reserve profiles used in this analysis represent potential reserve requirements, calculated based on worst-case forecast errors and statistical uncertainty margins. These values reflect the theoretical need for reserves to ensure system reliability under extreme or uncertain conditions. However, in practice, not all the reserve is procured, activated or utilized in real-time operations. The actual reserve activation is typically a fraction of the procured reserve capacity, depending on real-time imbalances, market dispatch signals, and grid conditions [5].

Therefore, while the analysis compares BESS contribution against the total estimated reserve requirement, this represents a conservative scenario, providing an upper bound on the flexibility and reliability needed from storage systems. The true operational role of BESS may vary depending on system operator strategies, market incentives, and real-time balancing needs.

#### 4.4 Monthly Analysis

To assess the operational behavior of the BESS across the year, a monthly breakdown of its contribution to both upward and downward reserves was carried out. This analysis provides insight into how seasonal variations in electricity prices, load patterns, and RES generation affect the profitability and feasibility of BESS participation in the reserve market. Figure 32 illustrates the number of hours per month in which BESS (i) contributed to the upward/downward reserve, and (ii) fully satisfied the system reserve requirement.

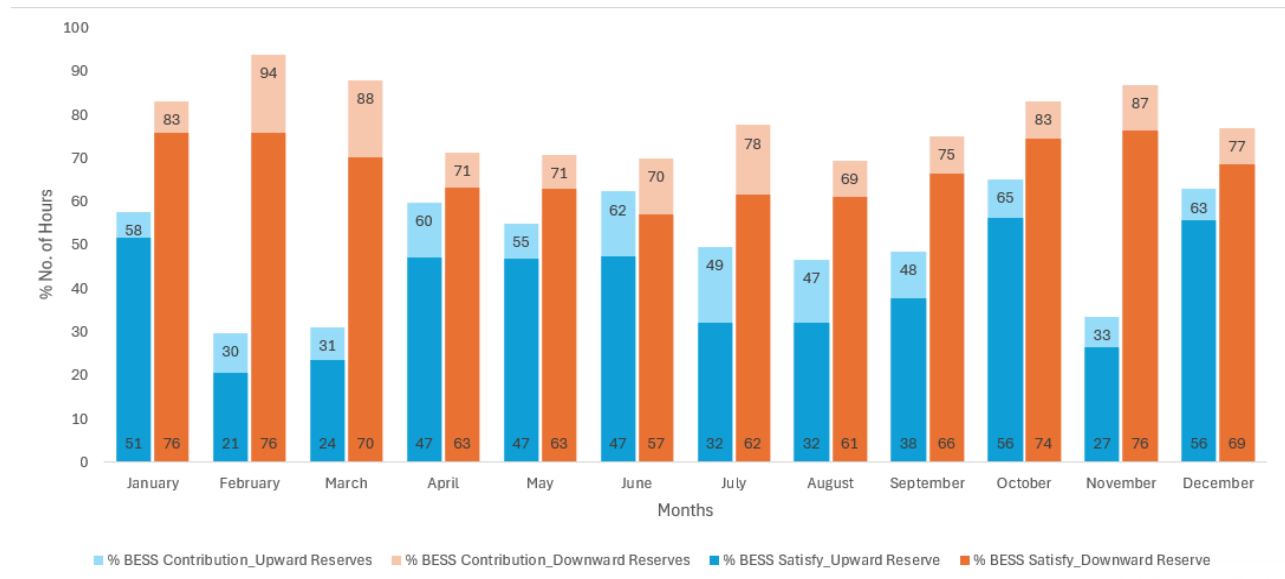


Figure 32. Monthly Analysis of BESS Contribution to Reserves

The monthly analysis shows that BESS more frequently contributes to downward reserves, with participation exceeding 65% (around 500 hours) in each month. This is a consequence of market-driven charging and discharging strategy that when prices are high, BESS discharges, reducing its SoC. This creates headroom to absorb energy, thereby enabling BESS to contribute to provision for downward reserves. Such price dynamics are particularly visible in winter months such as February where BESS is available to contribute around 94% (630 hours out of 672 hours) of the time in downward reserves while it has the potential to satisfy the downward reserve demand around 76% of the time. Similarly in March and November when BESS is available to contribute around 88% (654 hours out of 744 hours) and 87% (625 hours out of 720 hours) of the time while satisfying the demand around 70% and 76% of the time respectively. These are months where average prices tend to be

higher due to demand encouraging more discharging events following the time shifting strategy and thus increasing the capacity of BESS to participate in downward reserve provision.

In comparison, BESS participation in upward reserve provision varies more significantly across the year and is generally lower than for downward reserves. The ability to contribute to upward reserves depends on having sufficient stored energy (i.e., a high SoC), which is only possible if prior charging events were economically feasible. This condition is met more frequently in months like October, December and June where BESS is available to contribute around 65% (484 hours out of 744 hours), 63% (467 hours out 744 hours) and 62% (448 hours out of 720 hours) of the time respectively. It can also be noticed that the contribution of BESS to upward reserves is more consistent in the summer months, that is because of higher RES availability which leads to more charging events thus higher SoC.

Some Key Insights are as follows:

- **Downward Reserve Dominance:**

BESS consistently contributes more to downward reserves than upward reserves across all months. Contribution percentages for downward reserves exceed 70% in almost all months, with the highest seen in February (94%). This is primarily due to frequent discharge during high-price hours, which lowers SoC and creates space for charging. Additionally, in periods of low-RES availability, the system increasingly depends on BESS thus leading to higher market prices and ultimately discharge.

- **Satisfaction vs. Contribution:**

While contribution represents the hours BESS was available to provide reserve, satisfaction indicates whether BESS was capable of fully meeting the required reserve. Notably, in October and December, BESS has the potential to satisfy upward reserves demand in around 56% of the time. Downward satisfaction is even stronger, often above 60%, peaking at 76% in January, February and November.

- **Seasonal Patterns:**

In spring (April–June), BESS shows relatively high upward reserve contribution (55–62%), supported by increased RES availability and lower BESS demand. These conditions allow more frequent charging events, leading to higher SoC and better capability to contribute to upward reserves.

During summer (July–September), upward contribution slightly drops to (47-48%). However, satisfaction of downward reserves remains strong around 61-66%, indicating BESS continues to operate effectively in provision of downward reserves, even at high-RES availability.

Autumn and early winter (October–December) remain highly productive periods. October shows the highest upward contribution (65%) and strong satisfaction of downward reserves (74%), reflecting favorable market conditions, including sharp price spreads and adequate SoC. These months are likely to combine moderate RES generation with higher prices, optimizing both charging and discharging opportunities.

In late winter months (January–March), BESS performance is more mixed. In January, contribution to upward and downward reserves remains adequate, 58% and 83% respectively, suggesting balanced operation. In February, the downward contribution peaks at 94%, while the upward contribution drops to 30%, indicating that BESS frequently discharges due to high prices and low-RES availability, leaving it less available for upward reserves but highly effective at absorbing energy. March follows a similar pattern with a high downward contribution (88%) and relatively low upward availability (31%), again suggesting active discharging periods driven by market conditions and low-RES availability.

Overall, BESS behavior varies across seasons, driven by a combination of RES availability, demand patterns, and market price dynamics. This confirms the need for adaptive dispatch strategies that account for these seasonal shifts to maximize reserve support and profitability.

These insights can guide future market participation strategies and system planning, especially in shaping optimal dispatch patterns and storage sizing for future years.

#### 4.5 Weekend vs Weekday Analysis

To assess the influence of daily operational patterns on BESS participation, a comparative analysis was conducted between weekdays and weekends. The bar chart in Figure 33 presents the percentage total number of hours during which BESS is available to contribute and satisfy upward and downward reserve provision in each category.

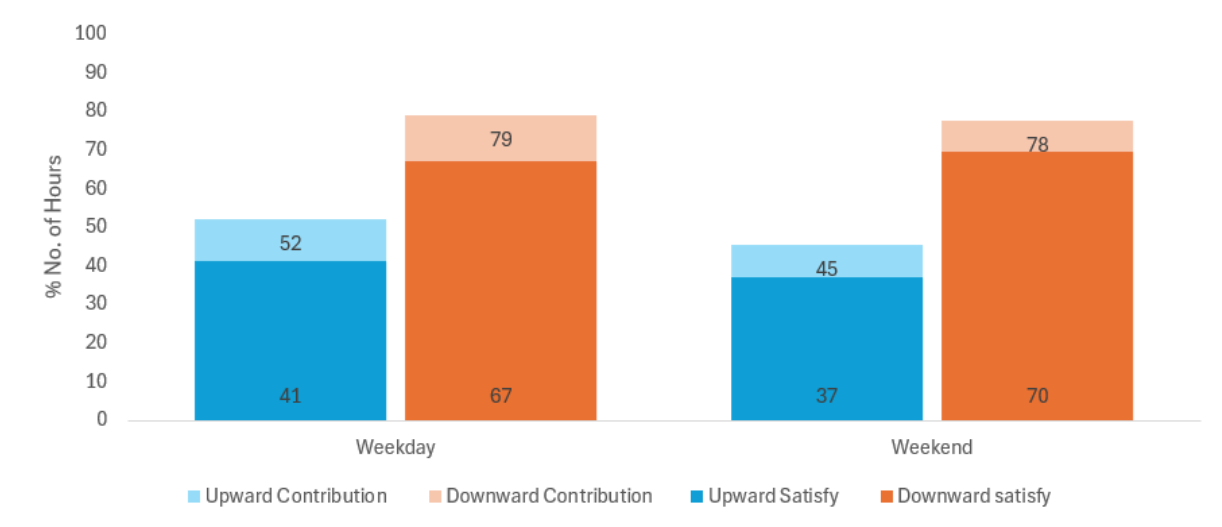


Figure 33. Weekend vs Weekday BESS Contribution to Reserve Requirement - 2030

The weekday vs. weekend analysis reveals a consistent pattern in BESS reserve behavior. On weekdays, BESS contributes to upward reserves during 52% of the hours and fully satisfies upward demand in 41% of the hours. Downward contribution and satisfaction are even more dominant, with BESS contributing 79% of the time and fully satisfying demand during 67% of the hours. At weekends, the trend remains similar but with slightly lower values: BESS contributes to upward reserves during 45% of the hours and satisfies them with 37%, while downward contribution and satisfaction remain high at 78% and 70%, respectively.

This performance gap between weekdays and weekends is linked to weekday load peaks and more frequent price fluctuations, which offer better charging/discharging opportunities and hence greater flexibility.

#### 4.6 Economic Analysis

This analysis evaluates the total reserve energy demand and its associated economic costs for 2030, considering automatic frequency restoration reserves (aFRR), spinning tertiary reserves (mFRR), and non-spinning tertiary reserves (RR Upward and RR Downward). The objective is to quantify the total reserve energy required, analyze the economic implications of its deployment, and assess seasonal variations in reserve costs. Economic costs were calculated adopting a possible future-proof approach based on capacity payment. We adopt an average reserve price of 1.76 €/MW/h, with the total yearly reserve cost obtained by summing the hourly costs, based on pilot experiences ongoing in Italy [32].

The reserve demand and economic analysis for 2030 provides critical insights into the evolving flexibility needs under a high-renewable penetration scenario. The total upward reserve requirement increases by almost 20%, from 41.48 TWh in 2023 to 51.41 TWh in 2030, while the downward reserve requirement rises by 38.45%, from 33.28 TWh in 2023 to 54.07 TWh in 2030. This sharp increase in downward reserves reflects the growing challenge of managing overgeneration due to large-scale renewable expansion, necessitating enhanced grid flexibility solutions as well as reducing dependency on thermal power plants. These numbers highlight the growing dependence on balancing mechanisms due to the variability of renewable generation.

The total yearly cost for upward reserves amounts to M€ 90.48, while downward reserves incur M€ 95.16, reflecting the financial burden of maintaining system flexibility. Notably, the cost of downward reserves represents payments to resources for being available to decrease their power output when required, rather than for the actual reduction itself. If downward reserves are activated, a separate payment (€/MW/h) is applied for reducing power generation. Namely, money is paid from the resources to the TSO for the reduced power generation with respect to the schedule. Currently, Italy follows a system where only energy activation is compensated, meaning that payments are made when power plants actively reduce generation. However, with the implementation of the Testo Integrato per il Dispacciamento Elettrico (TIDE<sup>2</sup>) framework [15], Italy is expected to transition towards a dual-payment system (capacity-based plus energy-based), aligning with common EU practices [33]. This system ensures that reserve providers are compensated not only for activation but also for their availability, improving grid reliability in a high-renewable scenario.

In this context, BESS emerge as a cost-effective and technically viable solution to meet a portion of these increasing reserve demands. Based on the modeled BESS participation in 2030, the system contributes to reserve provision during over 50% of the hours for upward reserves and nearly 79% for downward reserves. This significant level of involvement indicates that BESS can reduce dependency on thermal plants, which are typically more expensive and slower to respond. While BESS does not fully replace traditional reserve providers, it plays a critical role in shaving peak reserve needs, especially during periods of solar overgeneration, thereby minimizing the overcommitment of spinning or non-spinning reserves.

To estimate the economic cost of BESS, in 2023, the total reserve requirement (upward and downward combined) is calculated approximately 75.08 TWh. However, only 3.5 TWh of this reserve was activated [34] which corresponds to about 5% of the total reserve need. Assuming a similar activation percentage ratio applies in 2030 and given that the total reserve requirement for 2030 is 105.48 TWh, the expected volume of activated reserves would be 5.3 TWh (5% of 105.48 TWh).

From the model, the BESS is available to contribute 61.42 TWh out of the 105.48 TWh total reserve need, which is around 58%. If we apply the same share to the activated reserve volume, the BESS would be responsible for covering approximately 2.65 TWh (58% of 5.3 TWh) of the total activated reserves in 2030.

To calculate the cost, we use the LCOS, which is 50 €/MWh. However, LCOS is usually calculated only based on discharged energy, and does not fully account for the economic benefit BESS gains during charging periods; for instance, when it buys back energy at a lower price on the Day-Ahead Market (DAM). Since BESS provides value both while discharging (upward reserve) and charging

---

<sup>2</sup> TIDE (Testo Integrato per il Dispacciamento Elettrico) is a regulatory framework designed to enhance grid flexibility and market efficiency in Italy by introducing a dual-payment system for reserve capacity and activation, aligning with EU electricity market reforms.

(downward reserve), the cost is split equally between the two. Therefore, we apply  $LCOS/2 = 25$  €/MWh as a more realistic estimation. Applying this to the 2.65 TWh of activated reserves provided by BESS results in an estimated cost of approximately €66.25 million for reserve contribution by BESS in 2030. This cost estimate highlights the economic competitiveness of BESS as a reserve provider, especially under increasing system flexibility needs driven by renewable expansion. The ability of BESS to offer fast, decentralized, and low-carbon reserve support makes it a strategic asset for grid reliability and decarbonization. These findings can help inform policy decisions on future compensation schemes and investment planning for storage deployment.

## 5. Conclusions

This study presents a detailed assessment of reserve estimation methodologies for the Italian power system in 2030, addressing the challenges introduced by high renewable energy penetration and associated forecast uncertainties. Both formula-based and convolution-based methods were applied to quantify the reserve needs under different scenarios. The formula method, being more conservative, estimated a 20% increase in upward and a 38% increase in downward reserve requirements from 2023 to 2030, whereas the convolution method projected a lower increase (11.65% upward and 31.26% downward), highlighting the methodological impact on reserve planning. Given its conservative reliability, the formula-based approach was selected as the basis for BESS dispatch and economic modeling.

A system-level BESS model was implemented to assess its technical and economic role in meeting future reserve needs. The model demonstrated that BESS could contribute more than 50% of upward and nearly 80% of downward reserve hours, with the strongest contributions during months with high solar generation and favorable price conditions. The results confirm the strategic role of BESS in enhancing grid flexibility, especially during overgeneration or high-uncertainty periods. By absorbing excess energy and supporting peak demand, BESS reduces the reliance on conventional thermal units and mitigates the risk of curtailment.

Economically, a refined estimation method was used to evaluate the cost of BESS-based reserve provision. Assuming a 5% activation rate, BESS is expected to deliver approximately 2.65 TWh of reserve energy in 2030. Applying a split LCOS of €25/MWh (considering both upward and downward services), the estimated cost amounts to €66.25 million. This approach reflects a more realistic cost allocation and demonstrates that BESS can be a cost-effective contributor within an evolving capacity- and energy-based market design.

From a regulatory and planning perspective, this work provides valuable inputs for future ancillary service market design, including sizing BESS for reserve provision, evaluating compensation schemes under frameworks like TIDE, and encouraging availability-based remuneration. Although the study uses theoretical reserve needs and does not yet incorporate advanced forecasting improvements, it offers a robust technical and economic foundation for future reserve planning in high-renewable systems.

### 5.1 Future Recommendations

This study highlights several pathways to improve reserve estimation and system planning in high-renewables contexts like Italy. The choice between formula-based and convolution methods reflects a key trade-off: while the former ensures system security through conservative margins, it increases costs; the latter offers probabilistic flexibility but may risk under-procurement. A tailored risk-tolerance strategy is essential for balancing cost and reliability.

Future work should include real-time validation against Terna's actual balancing data, enabling dynamic refinement of reserve estimates. Adaptive reserve allocation based on real-time frequency trends, as implemented in Germany and the Netherlands [35]. Probabilistic scenario-based assessments, including Monte Carlo simulations, can help evaluate reserve adequacy under extreme events, aligning with best practices in the Nordic region [36]. Italy's system planning can benefit from similar stress-testing methodologies, ensuring that grid flexibility measures align with real-world uncertainty levels. Advanced forecasting techniques using AI and statistical tools like MAE and RMSE can also enhance reserve accuracy, with Germany and Denmark offering notable references which could serve as a valuable reference for Italy [37]. Finally, hybridizing methodologies using convolution under normal conditions and switching to formula-based sizing during stressed periods could yield both economic and operational benefits, complementing market-based ancillary service frameworks as seen in Spain and France [38].

While this study models BESS operation based on projected 2030 electricity prices and evaluates its contribution to system reserves, future research should focus on enhancing the market integration of BESS through advanced co-optimization frameworks. Such frameworks would enable batteries to simultaneously deliver multiple services such as reserve provision, energy arbitrage, and congestion management, thereby improving their economic viability. Recent research on dynamic stacking of multiple applications shows that optimized allocation of energy and power capacities across different services yields significant techno-economic benefits, particularly in Germany, where regulatory and technical conditions are evolving to support such multi-use models [39].

Furthermore, future modeling should explicitly incorporate battery degradation constraints and lifecycle-aware dispatch. Degradation-aware optimization algorithms, which account for opportunity costs due to battery wear, are increasingly recognized as essential for maximizing net present value and extending battery life, especially when BESS participates in high-frequency cycling services like reserves. Integrating these models ensures that operational strategies balance short-term revenue with long-term asset performance [40].

Italy's transition to the TIDE regulatory framework is expected to open new avenues for BESS to earn availability-based compensation, as practiced in other European countries. The introduction of mechanisms such as the MACSE 15-year tolling contracts will provide contracted revenue streams for BESS projects, incentivizing flexible capacity and ensuring state-of-charge availability during critical system hours even when energy arbitrage opportunities are limited. Future work should assess how these compensation schemes can further support the integration of storage into grid balancing and reliability services [20].

Finally, while this study uses historical price and load conditions to model BESS participation, more advanced approaches could employ stochastic optimization under multiple market scenarios to assess performance under uncertainty. Rolling-horizon and probabilistic models that dynamically update input information can increase the robustness of BESS operation against forecast errors and market volatility [41].

## References

- [1] “Global Energy Review 2025 – Analysis - IEA,” <https://www.iea.org/reports/global-energy-review-2025>.
- [2] IPCC, *Climate Change 2022 - Mitigation of Climate Change - Full Report*, no. 1. 2022.
- [3] E. C. Assessment and D. Operations, “Economic Cost-Benefit Assessment for Distribution Operations,” no. July, 2021.
- [4] G. Raimondi and G. Spazzafumo, “Integrating renewable energy communities and Italian UVAM project through renewable hydrogen chain,” *e-Prime - Adv. Electr. Eng. Electron. Energy*, vol. 10, Dec. 2024, doi: 10.1016/j.prime.2024.100819.
- [5] F. Bovera, G. Rancilio, D. Falabretti, and M. Merlo, “Data-driven evaluation of secondary-and tertiary-reserve needs with high renewables penetration: The Italian case,” *Energies*, vol. 14, no. 8, 2021, doi: 10.3390/en14082157.
- [6] M. A. Dubitsky, A. A. Rykova, and -Classification Of Power Reserves Of Electric Power Systems Rt&a # 01, “CLASSIFICATION OF POWER RESERVES OF ELECTRIC POWER SYSTEMS,” 2015.
- [7] I. Government, “Documento di Descrizione degli Scenari 2024,” *NA*, vol. 44, no. 8. pp. 1–14, 2011. doi: 10.1088/1751-8113/44/8/085201.
- [8] A. Ulbig, T. S. Borsche, and G. Andersson, “Impact of low rotational inertia on power system stability and operation,” in *IFAC Proceedings Volumes (IFAC-PapersOnline)*, 2014, vol. 19, pp. 7290–7297. doi: 10.3182/20140824-6-za-1003.02615.
- [9] C. Maurer, S. Krahl, and H. Weber, “Dimensioning of secondary and tertiary control reserve by probabilistic methods,” *Eur. Trans. Electr. Power*, vol. 19, pp. 544–552, May 2009, doi: 10.1002/etep.326.
- [10] Elia, “Methodology for the dimensioning of the aFRR needs,” pp. 1–80, 2020.
- [11] M. Matos *et al.*, “Probabilistic evaluation of reserve requirements of generating systems with renewable power sources: The Portuguese and Spanish cases,” *Int. J. Electr. Power Energy Syst.*, vol. 31, pp. 562–569, Oct. 2009, doi: 10.1016/j.ijepes.2009.03.031.
- [12] J. Wang, X. Chen, F. Zhang, F. Chen, and Y. Xin, “Building Load Forecasting Using Deep Neural Network with Efficient Feature Fusion,” *J. Mod. Power Syst. Clean Energy*, vol. 9, pp. 160–169, Jan. 2021, doi: 10.35833/MPCE.2020.000321.
- [13] L. Zhang, W. Huang, P. Kang, L. Zeng, Y. Zheng, and F. Zheng, “Configuration method of BESS in the wind farm and photovoltaic plant considering active and reactive power coordinated optimization,” *PLoS One*, vol. 16, Oct. 2021, doi: 10.1371/journal.pone.0257885.
- [14] M. S. Eltohamy, H. E. A. Talaat, M. S. A. Moteleb, S. F. Mekhamer, and W. A. Omran, “A Probabilistic Methodology for Estimating Reserve Requirement and Optimizing Its Components in Systems With High Wind Penetration,” *IEEE Access*, vol. 10, pp. 106148–106168, 2022, doi: 10.1109/ACCESS.2022.3211305.
- [15] “TIDE,” no. June, 2024.
- [16] Statista, “Largest thermal power plants operational in Italy.”
- [17] P. Technology, “Ostiglia Combined Cycle Power Plant Italy.” [https://www.power-technology.com/projects/ostiglia-combined-cycle-power-plant-italy/?utm\\_source=chatgpt.com](https://www.power-technology.com/projects/ostiglia-combined-cycle-power-plant-italy/?utm_source=chatgpt.com)
- [18] Enel Green Power, “Hydroelectric energy in Italy.” [Online]. Available: <https://www.enelgreenpower.com/learning-hub/renewable-energies/hydroelectric-energy/italy>
- [19] Enel Green Power, “Entracque hydroelectric plant, Italy.”
- [20] “Backup power for Europe - part 3: Italy’s bet on BESS - Rabobank,”

- <https://www.rabobank.com/knowledge/d011473382-backup-power-for-europe-part-3-italy-s-bet-on-bess>.
- [21] P. Giulia, "Long-term electricity price forecasting: merit order effect for 2030 in Italy," pp. 2024–2025, 2025.
- [22] RSE, "The Electricity Storage Capacity Procurement Mechanism (MACSE)," no. May, 2024, [Online]. Available: [https://www.rse-web.it/wp-content/uploads/2024/05/08\\_MACSE-inglese.pdf](https://www.rse-web.it/wp-content/uploads/2024/05/08_MACSE-inglese.pdf)
- [23] G. M. Francesca Tilli, "National Survey Report of PV Power Applications in Italy 2023," [https://iea-pvps.org/national\\_survey/national-survey-report-of-pv-power-applications-in-italy-2023/](https://iea-pvps.org/national_survey/national-survey-report-of-pv-power-applications-in-italy-2023/), 2024.
- [24] "Italy: wind power capacity 2023 | Statista," <https://www.statista.com/statistics/421815/wind-power-capacity-in-italy/>.
- [25] "Wind power in Italy: how much energy is produced and where," <https://www.enelgreenpower.com/learning-hub/renewable-energies/wind-energy/wind-power-italy>.
- [26] "Data Portal | Terna Driving Energy." <https://dati.terna.it/en/> (accessed Feb. 20, 2025).
- [27] M. Pozzi, G. Muliere, F. Fattori, M. Motta, and L. Mazzarella, "Electrification of Heat Demand: An Estimation of the Impact on the Future Italian Energy System," *J. Eur. des Syst. Autom.*, vol. 57, no. 5, pp. 1411–1417, 2024, doi: 10.18280/jesa.570516.
- [28] "Energy efficiency targets." [https://energy.ec.europa.eu/topics/energy-efficiency/energy-efficiency-targets-directive-and-rules/energy-efficiency-targets\\_en#final-2030-target](https://energy.ec.europa.eu/topics/energy-efficiency/energy-efficiency-targets-directive-and-rules/energy-efficiency-targets_en#final-2030-target) (accessed Feb. 20, 2025).
- [29] E. Nuno, M. Koivisto, N. A. Cutululis, and P. Sorensen, "On the Simulation of Aggregated Solar PV Forecast Errors," *IEEE Trans. Sustain. Energy*, vol. 9, no. 4, pp. 1889–1898, 2018, doi: 10.1109/TSTE.2018.2818727.
- [30] H. Holttinen *et al.*, *Design and operation of power systems with large amounts of wind power. Final summary report, IEA WIND Task 25, Phase three 2012-2014*. 2016.
- [31] J. Zhang, B. M. Hodge, and A. Florita, "Investigating the correlation between wind and solar power forecast errors in the western interconnection," *ASME 2013 7th Int. Conf. Energy Sustain. Collocated with ASME 2013 Heat Transf. Summer Conf. ASME 2013 11th Int. Conf. Fuel Cell Sci. Eng. Technol. ES 2013*, no. May, 2013, doi: 10.1115/ES2013-18423.
- [32] Terna, "Procedura di approvvigionamento a termine di risorse di dispacciamento per UVAM - Capacità assegnata per il periodo agosto 2024." <https://www.terna.it/it/sistema-elettrico/pubblicazioni/news-operatori/dettaglio/esitiastauvamagosto2024>
- [33] Frontier Economics, "Overview of European Electricity Markets," *EU Comm.*, no. February, p. 67, 2016.
- [34] "RELAZIONE INCENTIVO MSD," 2024.
- [35] M. Milligan and M. O. Malley, "Stochastic Methods for Planning and Operating Power System with Large Amounts of Wind and Solar Power Preprint," *11th Annu. Int. Work. Large-Scale Integr. Wind Power into Power Syst. as well as Transm. Networks Offshore Wind Power Plants Conf.*, no. September, 2012.
- [36] K. De Vos, N. Stevens, O. Devolder, A. Papavasiliou, B. Hebb, and J. Matthys-Donnadieu, "Dynamic dimensioning approach for operating reserves: Proof of concept in Belgium," *Energy Policy*, vol. 124, no. October 2018, pp. 272–285, 2019, doi: 10.1016/j.enpol.2018.09.031.
- [37] B. Eck, F. Fusco, R. Gormally, M. Purcell, and S. Tirupathi, "AI modelling and time-series forecasting systems for trading energy flexibility in distribution grids," *e-Energy 2019 - Proc. 10th ACM Int. Conf. Futur. Energy Syst.*, pp. 381–382, 2019, doi: 10.1145/3307772.3330158.
- [38] N. Viafora, S. Delikaraoglou, P. Pinson, G. Hug, and J. Holboll, "Dynamic Reserve and Transmission Capacity Allocation in Wind-Dominated Power Systems," *IEEE Trans. Power*

- Syst.*, vol. 36, no. 4, pp. 3017–3028, 2021, doi: 10.1109/TPWRS.2020.3043225.
- [39] S. Englberger, A. Jossen, and H. Hesse, “Unlocking the Potential of Battery Storage with the Dynamic Stacking of Multiple Applications,” *Cell Reports Phys. Sci.*, vol. 1, no. 11, Nov. 2020, doi: 10.1016/j.xcrp.2020.100238.
- [40] Z. Zhang, J. Shi, Y. Gao, and N. Yu, “Degradation-aware Valuation and Sizing of Behind-the-Meter Battery Energy Storage Systems for Commercial Customers.”
- [41] M. A. Hannan *et al.*, “Battery energy-storage system: A review of technologies, optimization objectives, constraints, approaches, and outstanding issues,” *J. Energy Storage*, vol. 42, Oct. 2021, doi: 10.1016/j.est.2021.103023.